Developmental Biology 430 (2017) 224–236

Contents lists available at ScienceDirect

Developmental Biology

journal homepage: www.elsevier.com/locate/developmentalbiology

# Expression and function of *spineless* orthologs correlate with distal deutocerebral appendage morphology across Arthropoda

Emily V.W. Setton[a], Logan E. March[a], Erik D. Nolan[a], Tamsin E. Jones[b], Holly Cho[a], Ward C. Wheeler[c], Cassandra G. Extavour[b,d], Prashant P. Sharma[a,*]

[a] Department of Integrative Biology, University of Wisconsin-Madison, 430 Lincoln Drive, Madison, WI 53706, USA
[b] Department of Organismic and Evolutionary Biology, Harvard University, 26 Oxford Street, Cambridge, MA 02138, USA
[c] Division of Invertebrate Zoology, American Museum of Natural History, Central Park West at 79th Street, New York, NY, USA
[d] Department of Molecular and Cellular Biology, Harvard University, 16 Divinity Avenue, Cambridge, MA 02138, USA

ARTICLE INFO

*Keywords:*
Homology
Selector gene
Morphological novelty
Appendages
Fate specification

ABSTRACT

The deutocerebral (second) head segment is putatively homologous across Arthropoda, in spite of remarkable disparity of form and function of deutocerebral appendages. In Mandibulata this segment bears a pair of sensory antennae, whereas in Chelicerata the same segment bears a pair of feeding appendages called chelicerae. Part of the evidence for the homology of deutocerebral appendages is the conserved function of *homothorax* (*hth*), which has been shown to specify antennal or cheliceral fate in the absence of Hox signaling, in both mandibulate and chelicerate exemplars. However, the genetic basis for the morphological disparity of antenna and chelicera is not understood. To test whether downstream targets of *hth* have diverged in a lineage-specific manner, we examined the evolution of the function and expression of *spineless* (*ss*), which in two holometabolous insects is known to act as a *hth* target and distal antennal determinant. Toward expanding phylogenetic representation of gene expression data, here we show that strong expression of *ss* is observed in developing antennae of a hemimetabolous insect, a centipede, and an amphipod crustacean. By contrast, *ss* orthologs are not expressed throughout the cheliceral limb buds of spiders or harvestmen during developmental stages when appendage fate is specified. RNA interference-mediated knockdown of *ss* in *Oncopeltus fasciatus*, which bears a simple plesiomorphic antenna, resulted in homeotic distal antenna-to-leg transformation, comparable to data from holometabolous insect counterparts. Knockdown of *hth* in *Oncopeltus fasciatus* abrogated *ss* expression, suggesting conservation of upstream regulation. These data suggest that *ss* may be a flagellar (distal antennal) determinant more broadly, and that this function was acquired at the base of Mandibulata.

## 1. Introduction

Homology, a shared correspondence or similarity as a result of common ancestry, is a key element of evolutionary inference. Historically, one of the grand challenges in comparative anatomy is the arthropod head problem, or the establishment of homologies for the segments and structures comprising the heads of arthropods (reviewed by Scholtz and Edgecombe (2006)). After over a century of debate, the positional homology of the deutocerebral (i.e., second head) segment of arthropods is generally accepted, based upon evidence from neuroanatomy (the innervation of the deutocerebral appendage pair by the deutocerebrum) and the boundaries of Hox gene expression, which is absent from the deutocerebral segment (Telford and Thomas, 1998; Hughes and Kaufman, 2002; Jager et al., 2006; Brenneis et al., 2008). Acceptance of this hypothesis was previously interpreted to mean that chelicerae are highly modified antennae or vice versa, but the markedly different architectures of antennae and chelicerae have historically hindered their direct comparison (Boxshall, 2004). We recently showed that RNA interference (RNAi)-mediated knockdown of *homothorax* (*hth*) in the harvestman *Phalangium opilio* results in homeotic chelicera-to-leg transformation (Sharma et al., 2015a), comparable to *hth* knockdown experiments in insects that result in antenna-to-leg transformations (Dong et al., 2001, 2002; Ronco et al., 2008). Therefore, homology of antennae and chelicerae is additionally substantiated by a shared fate specification program that involves (a) the absence of Hox signaling, and (b) a requirement for *hth* to confer appendage identity (Fig. 1).

Independently of genetic evidence, paleontological descriptions of

* Corresponding author.
*E-mail address:* prashant.sharma@wisc.edu (P.P. Sharma).

http://dx.doi.org/10.1016/j.ydbio.2017.07.016
Received 21 October 2016; Received in revised form 3 July 2017; Accepted 24 July 2017
Available online 29 July 2017

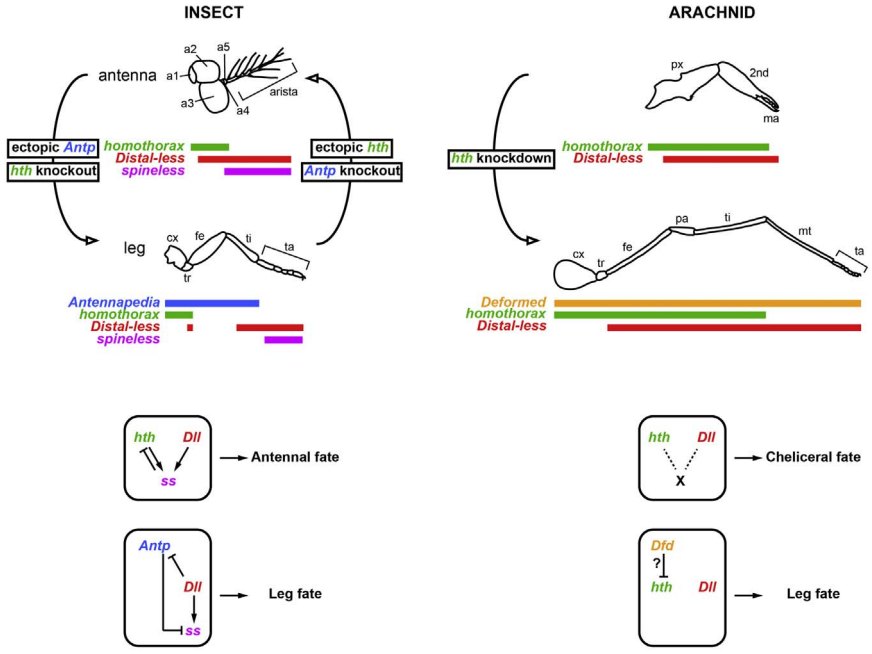


**Fig. 1.** Developmental dynamics of *hth* expression in deutocerebral and locomotory appendages of insects and arachnids (based on Duncan et al. (1998, 2010), Dong et al. (2001), Shippy et al. (2008), Toegel et al. (2009), Smith et al. (2014), and Sharma et al. (2015a)). Top left: Expression domains of *Antp*, *hth*, *Dll* and *ss* in the antenna and walking leg of *Drosophila melanogaster*. In *Drosophila*, *ss* is expressed in A2 through the arista. Labeled arrows indicate direction of homeotic transformation in misexpression experiments. Bottom left: Elements of the appendage fate specification pathway in *Drosophila*. Top right: Expression domains of *Dfd*, *hth*, and *Dll* in the chelicera and walking leg of *Phalangium opilio*. Note the absence of *Antp* in the leg bearing segments of arachnids. Bottom right: Elements of the appendage fate specification pathway in *Parasteatoda* and *Phalangium*. "X" denotes unknown cheliceral determinant/s.

Cambrian stem-group arthropods, concomitantly with improved techniques for fossil reconstruction and densely sampled phylogenies, have recorded early anterior appendages with multiple chelae (pincer-like claws) and multiple flagella (slender, articulated appendage termini corresponding to distal antennae). Such deutocerebral appendages are exemplified by leanchoiliids (an "antennate" megacheiran *sensu* Legg et al., 2013), which are part of the sister group lineage of extant Arthropoda (Megacheira; Chen et al., 2004; Legg et al., 2013; Siveter et al., 2014; Aria et al., 2015). These fossil appendages resemble neither modern chelicerae (which typically bear chelate terminal or subterminal segments, and dentition) nor modern antennae (which typically bear one or more flagella with numerous articles), but rather, a union of both appendage morphologies. Paleontologists have supported the deutocerebral origin of such appendages based on structural comparisons (Haug et al., 2012) and neuroanatomy in exceptionally preserved fossils (Ma et al., 2012; Tanaka et al., 2013; Yang et al., 2013; reviewed by Edgecombe and Legg (2014)). Given the phylogenetic placement of "Megacheira" in the arthropod tree of life as the paraphyletic sister group of crown-group Arthropoda (Daley et al., 2009; Kühl et al., 2009; Legg et al., 2013), reconstruction of deutocerebral appendage evolution is consistent with differential, lineage-specific retention of morphological features in Mandibulata and Chelicerata. However, other workers have inferred Megacheira to be more closely related to Chelicerata (Haug et al., 2012; Tanaka et al., 2013; Chipman, 2015); under this interpretation, the antenna would alternatively be constructed as a symplesiomorphic character.

The developmental genetic corollary of the hypothetical homology of antenna and chelicera is that downstream targets of *hth* may have also been retained in a lineage-specific manner, with modern mandibulates bearing determinants of flagellar identity, and chelicerates retaining the determinants of chela identity. To test the hypothesis that downstream targets of *hth* are lineage-specific, we examined the evolutionary dynamics of *spineless* (*ss*), a member of the bHLH-PAS family of transcription factors and homolog of the mammalian dioxin receptor (Struhl, 1982). In the larval antenna of the fruit fly *Drosophila melanogaster*, *ss* is initially co-activated by the proximo-distal (PD) axis patterning genes *hth* and *Distal-less* (*Dll*) in the distal territory of the antennal disc. By the third larval instar, *ss* represses *hth* in the distal antenna (Duncan et al., 1998). *ss* loss-of-function mutants display distal antenna-to-leg transformations, whereas ectopic expression of *ss* results in transformations of the maxillary palp and distal leg to distal antenna, and ectopic antennae in the rostral membrane (Duncan et al., 1998; Emerald and Cohen, 2004; Emmons et al., 2007). These data suggest that *ss* is the primary determinant of distal antennal fate in *D. melanogaster*.

Separately, *ss* is also expressed transiently and early (late second through third larval instars) in the tarsus of the *D. melanogaster* walking legs, and is required for activation of *bric-a-brac* and repression of *bowl*, two distally acting transcription factors that pattern tarsomeres (Godt et al., 1993; de Celis Ibeas and Bray, 2003). Loss-of-function mutants of *ss* display fusions or deletion of medial tarsomeres, and it has been suggested that *ss* acts to establish the tarsal field, which is subsequently partitioned into tarsomeres by *bric-a-brac* and *bowl* (Duncan et al., 1998; de Celis Ibeas and Bray, 2003).

Comparative work on the *ss* ortholog of the flour beetle *Tribolium castaneum* has shown conserved function of *ss* in patterning distal antennal identity, with respect to *D. melanogaster*. Both parental and larval RNAi against the *T. castaneum ss* ortholog result in transformation of a large region of the distal antenna to leg identity (Shippy et al., 2008; Toegel et al., 2009); in the tarsus, larval RNAi additionally results in tarsomere-patterning defects and truncation of the tarsus (Toegel et al., 2009; Smith et al., 2014).

Beyond these two holometabolous insects, expression and function of *ss* orthologs have not been investigated. Furthermore, extrapolating evolutionary scenarios from holometabolous insect models is complicated by the derived condition of both the antenna and the tarsus in these species. Holometabolous insects specify antennal identity at two points in development (during embryogenesis and metamorphosis), whereas hemimetabolous insects and non-insect hexapods specify antennal identity only once during embryogenesis (Shippy et al., 2008; Smith et al., 2014). With respect to tarsal morphology, the condition of five tarsomeres on the walking legs (four in the metathor-

acic leg of *T. castaneum*) is similarly a derived trait; a diverse group of hemimetabolous insects have two to three tarsomeres, and lineages near the base of Hexapoda have an undivided tarsus. Investigating the evolution of either appendage fate specification or tarsomere patterning in arthropods thus requires a representative of non-Holometabola.

Here we examined the expression and function of a *ss* ortholog in a hemimetabolous insect, *Oncopeltus fasciatus*. This species bears a plesiomorphic, simple antenna with four segments (scape, pedicel, and two flagellomeres), and the number of antennal segments is constant throughout post-embryonic growth. Similarly, *O. fasciatus* bears the plesiomorphic condition of three tarsomeres on all walking legs (but only two tarsomeres upon hatching), relative to Holometabola. To infer the evolutionary dynamics of *ss* across Arthropoda, we surveyed expression of *ss* orthologs of a crustacean, a centipede, a spider, and a harvestman. We demonstrate conservation of *ss* function in the antenna, but not the tarsus, of a hemimetabolous insect, and show that early expression of *ss* in the antennal limb buds evolved at the base of Mandibulata.

## 2. Materials and methods

### 2.1. Embryo cultivation and fixation

Adults of *Oncopeltus fasciatus* were maintained in a 28 °C animal facility at UW-Madison and fed ad libitum with crushed sunflower seeds. Dry cotton was used as egg-laying substrate and cohorts were separated by age using plastic boxes with vented lids. Embryos were fixed by briefly boiling eggs in 300 µl of deionized water and snap cooling on ice; washing in heptane; washing in methanol; and incubating in 4% formaldehyde in 1× PBS + 0.02% Tween-20 for 0.5–1 h prior to dehydration in methanol. Staging of *Oncopeltus* was based on number of hours after egg laying (AEL).

A colony of *Parhyale hawaiensis* adults at Harvard University was cultured at 28 °C in artificial seawater (Instant Ocean, Blacksburg, VA, USA) with crushed coral for substrate. Animals were fed daily with ground aquaculture feed: 40% TetraPond® wheat germ sticks, 40% TetraMin® flake food, and 20% Tropical® spirulina (Tetra, Blacksburg, VA, USA). Gravid females were anesthetized with $CO_2$, and embryos were collected by opening the brood pouch and flushing with sea water. Embryos were fixed by incubating in 3.7% formaldehyde in 1× PBS for 2 min at 75 °C, followed by 20 min in 3.7% formaldehyde in 1× PBS at 4 °C. Membranes were manually dissected from embryos in 1× PBS and embryos fixed overnight in 4% formaldehyde in 1× PBS + 0.02% Tween-20 at 4 °C, prior to dehydration in methanol. Staging of *Parhyale* followed Browne et al. (2005).

Adults of *Lithobius atkinsoni* were cultured in a 28 °C animal facility at UW-Madison. Breeding pairs were segregated in small containers with damp paper for substrate and fed twice per week with crickets. Eggs were collected every five days, soaked in water for 5–10 min, and the coating of debris manually removed with soft forceps. Embryos were then cultivated in a watchglass with damp paper until the desired stage. Embryos were fixed by dechorionation with 50% bleach diluted in deionized water for 1 min; several washes with 1× PBS; and incubating in 150 µL 5% formaldehyde in 1× PBS supplemented with 1.85 mL heptane, and agitation on a nutator 2 hr. Embryos were dehydrated in methanol prior to manual removal of membranes. Staging of *Lithobius* followed Kadner and Stollewerk (2004).

Adults of *Parasteatoda tepidariorum* were housed individually in a 28 °C animal facility at UW-Madison, using 175 mL plant containers with damp coconut fiber substrate and a foam lid for ventilation. Animals were fed every 3–4 days with live crickets. Young (first through fourth) cocoons were collected from webs and embryos maintained in watchglasses at 26 °C until the desired stage. Embryos were fixed by dechorionation with 100% bleach solution with agitation for 4–8 min; several washes with 1× PBS; and incubating in 5% formaldehyde in 1× PBS supplemented with heptane overnight on a platform shaker. Embryos were dehydrated in methanol prior to manual removal of membranes. Staging of *Parasteatoda* followed Mittmann and Wolff (2012).

Embryos of wild caught *Phalangium opilio* were obtained as described previously (Sharma et al., 2012a). Fixation of embryos followed the same protocol as for *Parasteatoda*, with longer wash steps to accommodate the larger embryos. Staging of *Phalangium* followed Sharma et al. (2012a).

### 2.2. Bioinformatics and phylogenetic analysis

Orthologs of *ss* were identified in genome projects of *Strigamia maritima* (Chipman et al. 2014), *Parasteatoda tepidariorum* (Schwager et al., 2017); and *Oncopeltus fasciatus* (Vargas Jentzsch et al. 2015); and from developmental transcriptomes of *Centruroides sculpturatus* (Sharma et al., 2015b), *Parhyale hawaiensis* (Zeng et al., 2011), *Phalangium opilio* (Sharma et al., 2014a), and *Lithobius atkinsoni* (this study). *Dmel-ss* (NCBI accession NP_001163629.2) and *Tcas-ss* (NCBI accession EEZ97710.2) were initially used as peptide sequence queries in tBLASTn searches, and hits with e-value $< 10^{-5}$ were retained. Putative orthologs were inferred using reciprocal BLAST, followed by multiple sequence alignment with MUSCLE v.3.8.31 (Edgar, 2004). Four vertebrate orthologs of the dioxin aryl hydrocarbon receptor, the vertebrate homolog of *ss*, were used to root the tree. Phylogenetic reconstruction consisted of maximum likelihood analysis with RAxML v.8.0 (Stamatakis, 2006) under the LG + Γ model, with 250 independent starts and 250 bootstrap resampling replicates (Stamatakis et al., 2008).

### 2.3. Cloning of orthologs and probe synthesis

Fragments of *ss* orthologs were cloned and Sanger sequenced for verification of transcriptomic assembly. PCR products were cloned using the TOPO® TA Cloning® Kit with One Shot® Top10 chemically competent *Escherichia coli* (Invitrogen, Carlsbad, CA, USA) following the manufacturer's protocol, and their identities verified by sequencing with the M13 universal primers. All primer sequences and amplicon lengths are provided in Supplementary File S1.

Probe synthesis was conducted using components of the MEGAscript® T7 kit (Ambion/Life Technologies, Grand Island, NY, USA). Templates for probe synthesis were made from plasmid templates using the M13 universal primers, following the manufacturer's protocol. Sense and anti-sense probes were synthesized using T7 and T3 RNA polymerases (Life Technologies, Grand Island, NY, USA) and precipitated with ammonium acetate, following the manufacturer's protocol. For *O. fasciatus* the largest available fragment was used for probe synthesis. For *P. tepidariorum*, the 5′ fragment was used for probe synthesis.

### 2.4. Whole mount in situ hybridization

Whole mount in situ hybridization for *O. fasciatus* was performed as described previously (Liu and Kaufman, 2009). Hybridization was performed at 55 °C with probe stock concentrations of 30 ng/µl prior to 1:10 dilution in hybridization solution. Staining reactions for detection of transcripts lasted between 0.5 and 1 h at room temperature. Embryos were subsequently rinsed with 1× PBS + 0.1% Tween-20 to stop the reaction, counterstained with 10 µg/mL Hoechst 33342 (Sigma-Aldrich, St. Louis, MO, USA) to label nuclei, post-fixed in 4% formaldehyde in 1× PBS + 0.1% Tween-20, and stored at 4 °C in glycerol.

Whole mount in situ hybridization for *P. hawaiensis* was performed as described previously (Rehm et al., 2009) with the following modifications: prior to rehydration, embryos were cleared by incubation in xylene for 20 min. Hybridization was performed at 67 °C with

probe stock concentrations of 30 ng/μl prior to 1:10 dilution in hybridization solution. Following post-fixation, embryos were incubated in detergent solution (1.0% SDS, 0.5% Tween, 50.0 mM Tris–HCl (pH 7.5), 1.0 mM EDTA (pH 8.0), 150.0 mM NaCl) for 30 min and then fixed again in 3.7% formaldehyde for 30 min. After hybridization, embryos were washed twice in 2× saline sodium citrate for 30 min and then twice in 0.2× saline sodium citrate for 30 min. Staining reactions for detection of transcripts were run overnight at 4 °C.

In situ hybridization for *P. tepidariorum* and *P. opilio* followed published protocols (Akiyama-Oda et al., 2003; Sharma et al., 2012a), with probe stock concentrations of 300–400 ng/μl prior to a 1:10 dilution in hybridization solution. A published protocol was also followed for *L. atkinsoni* (Kadner and Stollewerk, 2004), with probe stock concentrations of 400 ng/μl prior to a 1:10 dilution in hybridization solution. Staining reactions for detection of transcripts lasted between 0.5 and 6 h at room temperature. Embryos were subsequently rinsed with 1× PBS + 0.1% Tween-20 to stop the reaction, counterstained with 10 μg/mL Hoechst 33342 (Sigma-Aldrich, St. Louis, MO, USA) to label nuclei, post-fixed in 4% formaldehyde in 1× PBS + 0.1% Tween-20, and stored at 4 °C in glycerol.

All probes were visualized using nitro-blue tetrazolium (NBT) and 5-bromo-4-chloro-3′-indolyphosphate (BCIP) staining reactions. Embryos were mounted in glycerol and images were captured using a Nikon SMZ25 fluorescence stereomicroscope mounted with either a DS-Fi2 digital color camera or a Q-Imaging digital monochrome camera, driven by Nikon Elements software.

### 2.5. Double-stranded RNA synthesis and RNA interference

Double-stranded RNA (dsRNA) was synthesized with the MEGAscript® T7 kit (Ambion/Life Technologies, Grand Island, NY, USA) from amplified PCR product (above), following the manufacturer's protocol. The synthesis was conducted for 4 h, followed by a 5 min cool-down step to room temperature. A LiCl precipitation step was conducted, following the manufacturer's protocol. dsRNA quality and concentration were checked using a Nanodrop One spectrophotometer (Thermo Scientific, Wilmington, DE, USA) and the concentration of the dsRNA was subsequently adjusted to 2 μg/μl with 1× *Tribolium* injection buffer for *O. fasciatus*, and 4 μg/μl with deionized water for *P. tepidariorum*.

*O. fasciatus* in the last nymphal stage were isolated and segregated by sex upon their final molt into adulthood. Three days after the final molt, 16 virgin females were anesthetized using $CO_2$ and injected with 10 μg of dsRNA of an 798-bp fragment of *Ofas-ss* (13 females survived injections). As a negative control, 11 females were injected with an equal volume of 1× *Tribolium* injection buffer (nine females survived injections). Injected females were housed individually with a single wild type male and egg clutches collected every day from dry cotton substrate. Development was followed until egg hatching, and hatchlings were fixed in 96% ethanol. Hatchlings were subsequently scored as wild type (normal development), dead (failure to hatch), indeterminate (could not be scored due to damage to appendages), or one of three phenotype classes ranked by severity (criteria provided in Results). Hatchlings were imaged both using a Nikon SMZ25 fluorescence stereomicroscope and a Zeiss EVO 50 scanning electron microscope (SEM).

To rule out off-target effects, dsRNA was synthesized for injection as two additional non-overlapping *Ofas-ss* fragments of similar size (447 and 428 bp), with each injected into five females. Females injected with smaller fragments were maintained as described above, and the first six clutches were collected. Internal primer sequences of *Ofas-ss* are provided in Supplementary File S1.

To test whether the regulatory interaction between *ss* and *hth* is conserved outside of Holometabola, pRNAi was conducted against *Ofas-hth*. Fourteen virgin females were injected with a 594 bp fragment of *Ofas-hth* dsRNA (11 females survived), with another eight females injected with 1× *Tribolium* buffer (six females survived). A subset of the resulting embryos was developed to 5–6 days AEL to identify clutches with clear *hth* loss-of function phenotypes, and the remaining embryos were fixed at 62–72 h AEL and assayed for expression of *Ofas-ss* via in situ hybridization.

Adult virgin females of *P. tepidariorum* were injected every other day along the lateral surface of the opisthosoma (i.e., posterior tagma of chelicerates), for a total 32 μg dsRNA delivered over four injections. Two non-overlapping fragments of *Ptep-ss-1* and a single (5′) fragment of *Ptep-ss-2* were targeted for knockdown (four-five virgin females per fragment). To rule out compensatory effects of the two paralogs, dsRNA was also injected targeting both paralogs simultaneously; three females were injected with the 5′ fragment of both *Ptep-ss* paralogs, and another three females with the 3′ fragment of both *Ptep-ss* paralogs. For the double knockdowns, the concentration by mass of the dsRNA was adjusted to be equal, and a total of 16 μg dsRNA was delivered for each paralog over four injections. As negative controls, seven females were injected with an equal volume of deionized water, following Khadjeh et al. (2012). A single fragment of *Ptep-Distal-less* was injected as a positive control into three females (see Pechmann et al., 2011). Females were fed and mated 18–24 h after the last injection and the first five cocoons were collected.

### 2.6. Verification of gene knockdown

To verify knockdown of *ss* in *O. fasciatus*, we injected a separate group of virgin females with the 5′ 467-bp fragment of *Ofas-ss* and with 1× *Tribolium* buffer. We preserved 15 eggs from the third and fourth clutches of each female at 72 h AEL in TRIzol (Invitrogen) at −80 °C, and permitted the remainder of the clutches to complete development. Phenotypes were scored upon hatching. We selected clutches from the female with the highest proportion of class III phenotypes, in addition to clutches of a buffer-injected female, and completed RNA extractions following the manufacturer's protocols. Total RNA concentration was adjusted to 300 ng/μl using a NanoDrop ONE (ThermoScientific) prior to cDNA synthesis. First-strand cDNA was prepared using oligo(dT) primers and SuperScript III reverse trancriptase (Invitrogen). The cDNA was used as a template for qPCR reactions. Two endogenous controls were used for relative quantitation of gene expression, FoxK and elongation factor 1α (EF1α). Quantitative PCR (qPCR) was conducted using PowerUp SYBR Green Master Mix (Life Technologies) on a StepOne Plus Real-Time PCR instrument (Applied Biosystems) using the manufacturer's Fast protocol. Results were analyzed using StepOne Plus software (Applied Biosystems). All primer sequences and target amplicon lengths are provided in Supplementary File S1.

Penetrance of RNAi in *P. tepidariorum* is empirically highly variable, and many studies have reported large subsets of clutches to retain the wild type phenotype upon pRNAi (e.g., Turetzek et al., 2015). Consequently, knockdown of *ss* orthologs in *Parasteatoda* was verified solely using in situ hybridization.

## 3. Results

### 3.1. Identification of arthropod ss orthologs

After culling 5′ and 3′ hanging ends, the multiple sequence alignment of *ss* homologs retrieved from transcriptomic and genomic databases consisted of 883 amino acid sites (Supplementary File S2). The maximum likelihood tree topology recovered the monophyly of putative *ss* homologs with maximal nodal support (Fig. 2A), with basal topology of the arthropod *ss* gene tree in accord with basal arthropod phylogeny (Campbell et al., 2011; Borner et al., 2014). Single copy orthologs were recovered for all species except *P. tepidariorum* and *C. sculpturatus*, which bore two paralogs distinguished by 91 non-synonymous substitutions, in addition to eight indel events (73.6%

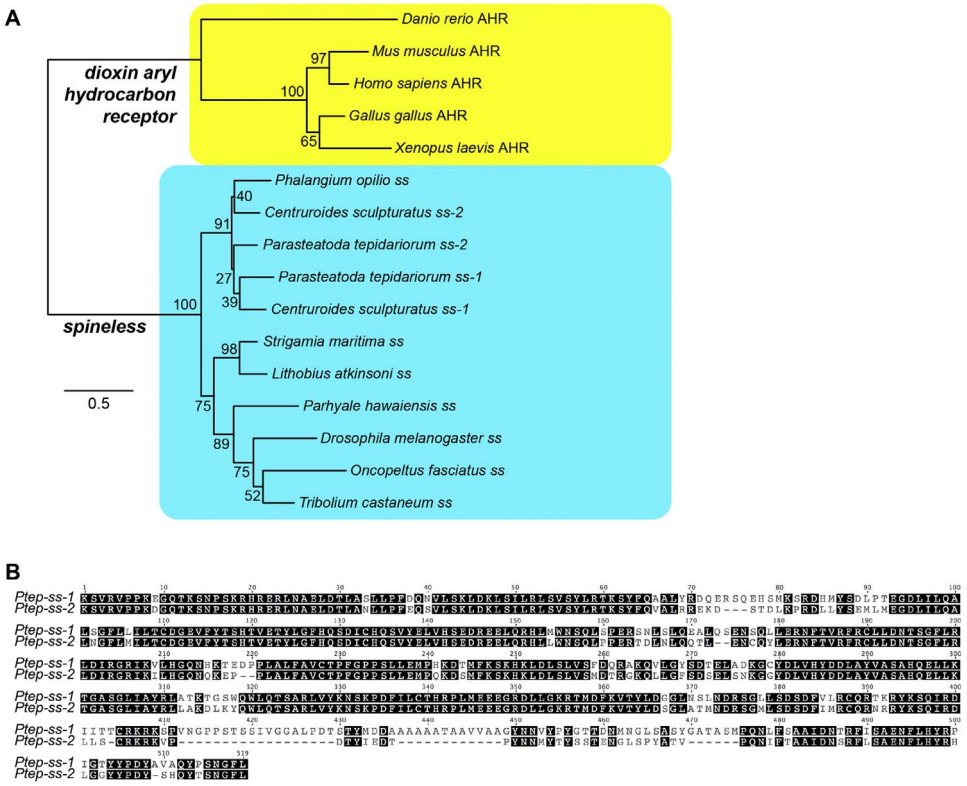


**Fig. 2.** (A) Maximum likelihood tree topology of arthropod *spineless* orthologs (ln*L* = −12257.99). Numbers on nodes indicate bootstrap resampling frequencies. (B) Peptide alignment of spider *ss* paralogs. Black shading indicates identical sites.

pairwise identity in peptide alignment; Fig. 2B). We refer to the long and short *Ptep-ss* homologs as *Ptep-ss-1* and *Ptep-ss-2*, respectively.

### 3.2. Expression of ss orthologs in Mandibulata

In *Oncopeltus*, strong *Ofas-ss* expression was observed in the limb buds of the antennal segment during germ band elongation. At 62 h AEL, no expression was observed in body segments posterior to the antennal (deutocerebral) segment (Fig. 3A). During appendage outgrowth (72–76 h AEL), strong *ss* expression was retained in the elongating antennal limb buds (Fig. 3C, D). We did not detect expression in the termini of the walking leg, the maxilla, or the labium. Due to non-specific staining in the termini of maxillary and labial outgrowths in later (> 80 h AEL) developmental stages (Fig. 6B), we were unable to assess *ss* expression in these appendages in later stages. No expression was detected using a sense probe at corresponding stages (Fig. 3B), suggesting that the antennal expression of *Ofas-ss* is specific.

In *Parhyale* embryos, expression of *Phaw-ss* was first detected at stage 18 as faint expression in the medial antennal buds and at the bases of some trunk appendages (not shown). Strong and clear expression was first observed at stage 19, with *Phaw-ss* detected in a medial band in the first (deutocerebral) antennal limb bud, with weaker expression in the distal part of this appendage; more homogeneous expression throughout the distal part of the second (tritocerebral) antennal limb bud; in both pairs of maxillae; and at the coxa-trochanter joints of posterior trunk appendages (Fig. 3E). By stage 21, more homogeneous *Phaw-ss* expression was detected throughout the flagellum (the distal component) of both antennal pairs, with no expression in the proximal-most segments of these appendages (Fig. 3F). In addition, a pair of small expression domains was observed in the head lobes anterior to both antennal pairs. In posterior segments, expression was observed in the coxa-trochanter joints of posterior trunk appendages, as well as in dot-like patterns in lateral ectodermal tissue (Fig. 3G). No expression was detected in the sense probe of corresponding stages (not shown).

In *Lithobius*, expression of *Latk-ss* was only observed in the limb buds of the antennal segment in stage 4 and 5 embryos (Fig. 3H). No expression was detected in the sense probe of corresponding stages (not shown).

### 3.3. Expression of ss orthologs in Chelicerata

None of the arachnid *ss* orthologs was expressed throughout the cheliceral limb bud during embryogenesis.

The two paralogs of *ss* in the spider *Parasteatoda* were distinguished both positionally and temporally. The longer paralog, *Ptep-ss-1*, was initially weakly expressed in stage 9.2 embryos at the base of the cheliceral limb buds, in the termini of the palps and walking legs, and in the posterior part of the O4 and O5 opisthosomal segments, corresponding to the primordia of the anterior and posterior spinnerets, respectively (Fig. 4A, B). In the prosoma of later stages (stages 10.1–10.2), *Ptep-ss-1* was expressed in a dorso-medial region of the chelicerae; in the gnathendites of the pedipalp and all walking legs; and as dots of expression in the tibiae through the tarsi of the pedipalp and all walking legs (Fig. 4C). In the pedipalp and leg tarsi, density of expression increased significantly in the tarsal field, but was absent from the distal terminus of the tarsus. In the opisthosoma of stage 10.2 embryos, strong expression of *Ptep-ss-1* was detected in the spinneret buds, with a single region of expression within the primordia of the anterior spinneret pair, and three discrete regions of expression in the posterior spinneret pair (Fig. 4D, E).

Expression of the shorter paralog, *Ptep-ss-2*, was not detected prior to stage 11. In the prosoma of stage 11 embryos, *Ptep-ss-2* was detected in the tarsi of the pedipalp and all walking legs as weak dots of expression, relative to *Ptep-ss-1* (Fig. 4F). As with *Ptep-ss-1*, expression of *Ptep-ss-2* was absent from the distal terminus of the tarsus. No expression was observed in gnathendites at this stage. In the

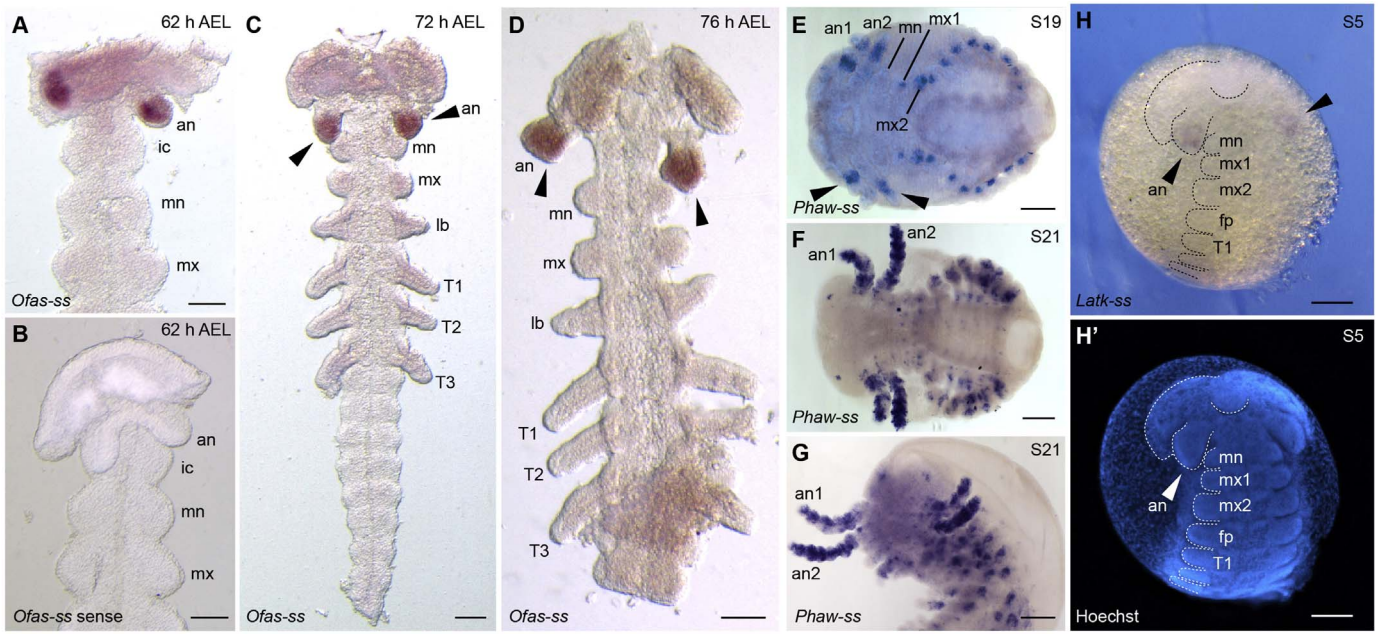


**Fig. 3.** Expression of *ss* orthologs across Mandibulata is associated with distal antennae (flagella). In *Oncopeltus* (A-D), *Ofas-ss* is expressed in the antennal limb buds (A). No expression of the sense probe of *Ofas-ss* is detected in the corresponding stage (B). *Ofas-ss* continues to be strongly expressed in the antennal limb buds (arrowheads) through germ band elongation (C-D). In *Parhyale* (E-G), at stage 19 *Phaw-ss* is expressed in the distal parts of both antennal pairs (arrowheads), both maxillary pairs, and at the base of posterior trunk appendages (E). By stage 21 (F, G) *Phaw-ss* is expressed throughout the flagellum of both antennal pairs, which have formed antennomeres. Dots of *Phaw-ss* expresssion are also observed in the head lobes and in peripheral tissue in posterior segments (F, G). In *Lithobius* (H) *Latk-ss* is expressed in the antennal limb buds (arrowhead), comparably to early stages of insects. (H′) Counterstaining of (H) with Hoechst 33342. Abbreviations: an: antenna; an1: crustacean deutocerebral antenna; an2: crustacean tritocerebral antenna; fp: forcipule; ic: intercalary segment; lb: labium; mn: mandible; mx1: first maxilla; mx2: second maxilla; T1: first thoracic appendage. Black arrowheads indicate antennal expression. Scale bars: 100 μm (A-G); 200 μm (H).

opisthosoma of stage 11 embryos, *Ptep-ss-2* was detected in both spinneret pairs, but with stronger expression in the anterior spinnerets than in the posterior spinnerets, and without discrete expression domains within the posterior spinneret (Fig. 4G). The comparatively restricted and weak expression of *Ptep-ss-2* with respect to *Ptep-ss-1* in the pedipalp and leg tarsi was consistently observed until later stages, when the tarsal expression of *Ptep-ss-2* became stronger and broader relative to earlier stages (compare Fig. 4H to F).

The single *ss* ortholog of *Phalangium* was initially expressed in stage 12 embryos in the gnathendites of the walking legs (Fig. 4I). Comparably to *Ptep-ss-1*, expression of *Popi-ss* in later stages encompassed a dorso-medial region of the chelicerae, and the gnathendites and tarsi of the pedipalps and all walking legs pairs (Fig. 4J). In the pedipalp of stage 15 embryos *Popi-ss* was strongly expressed as a solid band in the tarsus, and as rings at the distal end of the patella and tibia. Expression was also detected in the posterior terminus of the embryo. Intriguingly, the elongating tarsi of harvestman walking legs expressed different numbers of bands of *Popi-ss*, with the most bands observed in the second walking leg (Fig. 4K). These patterns correlate with the number of tarsomeres that occur in each leg pair; walking legs with more tarsomeres in the first postembryonic stage bore additional bands of *Popi-ss* expression. The exact correlation could not be established, because late-stage accumulation of cuticle in the distal walking legs precludes a count of the final number of *Popi-ss* expression rings in stages prior to hatching.

### 3.4. Parental RNA interference in O. fasciatus

Across the first eight clutches of eggs laid by *Oncopeltus* females injected with a 798-bp fragment of *Ofas-ss*-dsRNA, 71.3% (N = 900/1263) of eggs hatched successfully, and of these, 70.4% (N = 634) displayed homeotic defects in the distal antennae, as inferred from the presence of tarsal claws at the distal terminus of the antenna and the absence of sensilla basiconica (sensory structures unique to the distal-most segment of the wild type antenna) in the transformed appendages (Fig. 5). In buffer-injected negative controls, the proportion of eggs that hatched successfully was similar (79.9%; N = 963). In late stage embryos with homeotically transformed distal antennae, we confirmed reduced expression of *Ofas-ss* (Fig. 6B).

We classified hatchlings with mostly unaffected antennae that bore a pair of tarsal claws at the distal terminus of the second flagellomere (fg2) as Class I phenotypes (N = 247; Figs. 5, 6D). Hatchlings with a shorter and thicker fg2 were classified as Class II phenotypes (N = 208; Figs. 5, 6D). Class III phenotypes (N = 179; Figs. 5, 6D) were further distinguished in the spectrum of phenotypes by a point of inflection in the middle of fg2, and a variably developed segmental boundary at the inflection; we interpret this phenotype to correspond to the boundary between the first and second tarsomeres (ta1 and ta2) in the walking leg. We were not able to establish which walking leg (T1, T2, or T3) identity was patterned in the antenna in the knockdown experiments, as markers of leg identity (e.g., the tibial spines of the T1 leg) were not induced in the distal antenna-to-leg transformations. No morphological difference was detected in the walking legs of Class I-III hatchlings with respect to wild type walking legs. Specifically, the morphology of ta1 and ta2 was unaffected (Fig. 5).

We observed the same phenotypes when injecting either of two non-overlapping fragments of *Ofas-ss* (Fig. 6A; Supplementary File S3). Relative gene expression as assessed by qPCR indicated 77% expression in clutch three, and 81.1% expression in clutch four, with respect to buffer injected controls; 100% of other individuals from these clutches that hatched displayed Class III phenotypes (Fig. 6E).

### 3.5. Inference of Ofas-ss regulation

Knockdown of *Ofas-hth* resulted in a range of phenotypes previously reported by Angelini and Kaufman (2004) (Fig. 7). Specifically, upon knockdown of *Ofas-hth*, we observed in late stage embryos a range of segmentation defects along the AP axis, as inferred from the

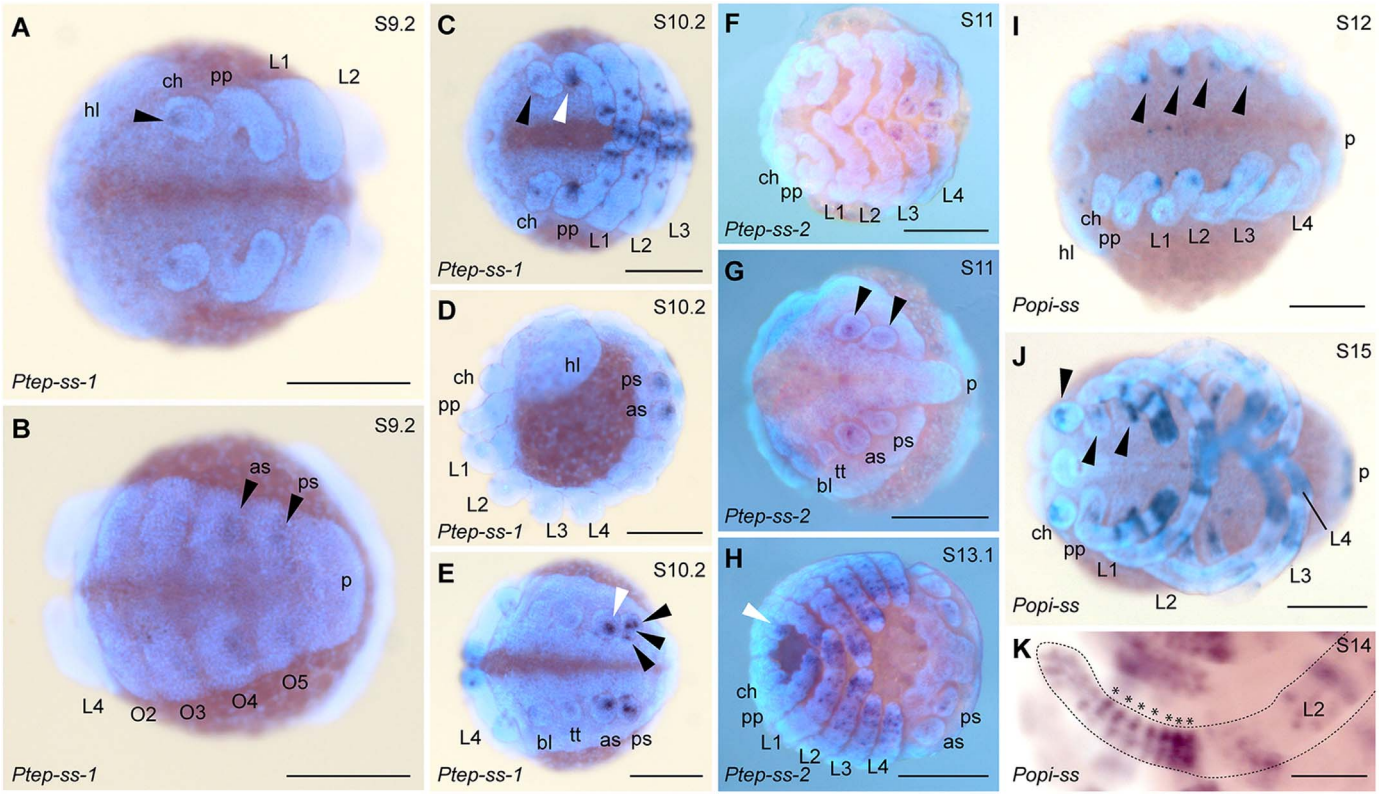


**Fig. 4.** *ss* orthologs of Chelicerata are not expressed throughout the distal chelicera. Two *ss* paralogs occur in *Parasteatoda* (A-H). *Ptep-ss-1* initially detected in stage 9.2, with expression domains in the base of the chelicera (A) and in the posterior of the O4 and O5 opisthosomal segments (B). Black arrowheads in (A) and (B) indicate faint expression domains. In the prosoma of stage 10.2 embryos (C), *Ptep-ss-1* is expressed in a dorso-medial field in the chelicera (black arrowhead), in the gnathendites of the posterior appendages (white arrowhead), and as dots of expression concentrated in the tarsi of the pedipalps and walking legs. In the opisthosoma (D-E), prominent expression is observed in the spinneret primordia (D). (E) Multiple discrete expression domains occur within the posterior spinneret (black arrowheads), whereas a single, larger expression domain occurs in the anterior spinneret (white arrowhead). Expression of *Ptep-ss-2* is not detected until stage 11 (F), with weak spots of expression in the pedipalpal and walking leg tarsi. In the opisthosoma of stage 11 embryos (G), *Ptep-ss-2* is faintly expressed in the spinneret primordia (black arrowheads), with a single expression domain in both spinneret pairs. By stage 13.1 (H), stronger dots of *Ptep-ss-2* expression occur in the distal pedipalp and walking leg podomeres, but are absent from the distalmost part of the tarsus. Additional expression domains occur in the gnathendites (white arrowhead). A single ortholog of *ss* was discovered in the harvestman (I-K). Onset of *Popi-ss* expression occurs in the walking leg gnathendites of stage 12 embryos (I). Additional expression domains of *Popi-ss* in later stages include a dorso-medial field in the chelicera, the posterior terminus, the tarsi of the pedipalp and the walking legs, and stripes of expression at the distal end of the pedipalpal patella and tibia (J). In the walking leg tarsus (K), the number of stripes of *Popi-ss* expression correlates with the number of tarsomeres that will occur in the hatchling, with the most stripes (asterisks) in the developing second walking leg. Abbreviations: as: anterior spinneret; bl: book lung; ch: chelicera; hl: head lobe; L1: first walking leg; p: posterior terminus; ps: posterior terminus; pp: pedipalp; tt: tubular trachea. Scale bars in A-J are 200 μm; scale bar in K is 100 μm.

overall length of the embryo and the number of spiracles along the pleural margin (Fig. 7C, D); appendage truncation and appendage fusion (Fig. 7E); and reduction of the eyes (Fig. 7C). From a subset of three females injected with *Ofas-hth*-dsRNA, whose pre-hatchlings displayed previously described *Ofas-hth* loss-of-function phenotypes, embryos from seven clutches were surveyed for *Ofas-ss* expression via in situ hybridization. Of 14 embryos examined that displayed clear *hth* loss-of-function phenotypes at 72 h AEL, none displayed any detectable expression of *Ofas-ss*, compared to 100% of embryos from buffer-injected females (Fig. 7B, E). We interpret these data to suggest that a positive regulatory interaction of *ss* by *hth* is conserved in Holometabola and *O. fasciatus*.

### 3.6. Parental RNA interference in P. tepidariorum

In *P. tepidariorum*, no effect on cheliceral morphology was observed upon individual knockdown of either *Ptep-ss-1* (both 5′ and 3′ fragments) or *Ptep-ss-2* (5′ fragment only), or joint knockdown of both *Ptep-ss-1* and *Ptep-ss-2* (both 5′ fragments and both 3′ fragments, N > 800 for every experiment; Supplementary Fig. 1A-1K); all embryos and hatchlings examined displayed wild type morphology of the chelicerae and walking leg tarsi (as in Supplementary Fig. 1L).

For single-paralog knockdowns, no expression signal of the target gene was detectable with in situ hybridization for either *Ptep-ss-1* and *Ptep-ss-2* (Figure Supplementary Fig. 1D, 1E). For double-paralog knockdowns, we observed some weak expression signal in the second clutch, and degradation of detectable signal through progression to clutch four (Supplementary Figure 1F-1K), consistent with previous *P. tepidariorum* pRNAi experiments (e.g., Khadjeh et al., 2012). All first ("post-embryo") and second instars displayed wild type morphology with respect to the chelicera, the tarsi of the pedipalps, the "maxilla" (gnathendite) of the pedipalps, the walking legs, and the spinnerets. By contrast, in the *Distal-less* (*Dll*) positive control injections, > 90% (N = 428) of hatchlings from the second through fourth clutches (pooled data from two surviving females) displayed a previously reported gap phenotype (six-legged spider hatchlings, Pechmann et al., 2011; Supplementary Fig. 1M), with the rest of the clutch displaying a mosaic gap phenotype (seven legs) or wild type (eight legs) morphology (Supplementary File S4).

## 4. Discussion

### 4.1. Retention and copy number of ss orthologs

Single copy orthologs of *ss* were discovered in all mandibulates and the harvestman *Phalangium opilio*. By contrast, two copies of *ss* were discovered in the genome of *Parasteatoda tepidariorum* and in the developmental transcriptome of *Centruroides sculpturatus*, which

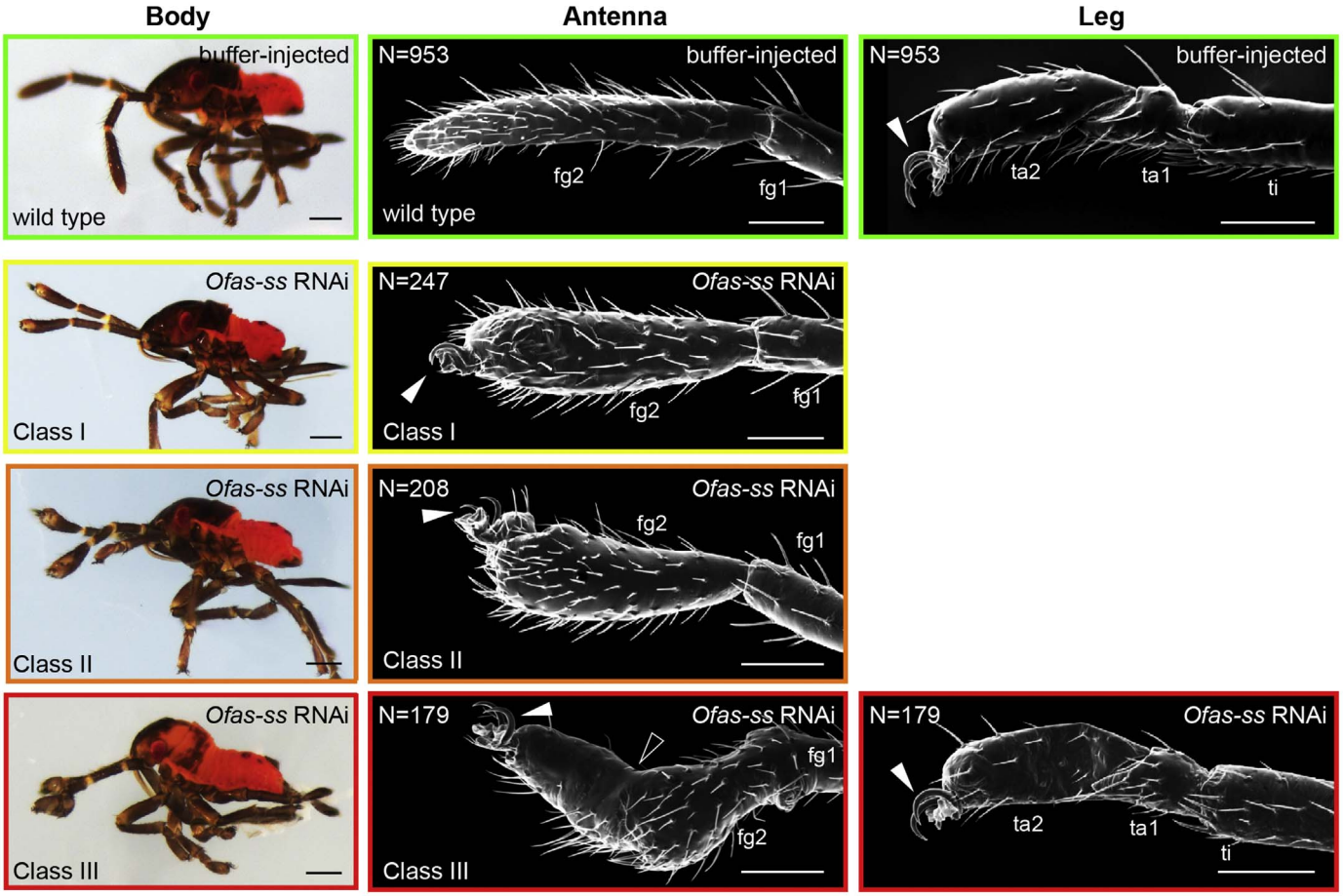


**Fig. 5.** Parental RNA interference against *Ofas-ss* showing morphology of *Oncopeltus* first instar hatchlings; wild type (green panels), Class I (yellow panels), Class II (orange panels), and Class III (red panels) phenotypes. Left column: whole body in lateral view. Middle column: SEM micrographs of distal antenna. Right column: SEM micrographs of walking leg I tarsus. White arrowheads indicate tarsal claws. Black arrowhead indicates point of inflection in homeotically transformed distal antenna of class III hatchlings. Abbreviations: fg1: flagellomere 1; ta1: tarsomere 1; ti: tibia. Scale bars in left column of (B) are 200 μm; scale bars in middle and right columns in (B) are 100 μm.

differed significantly in sequence length, sequence composition, gene expression domain, and onset of embryonic gene expression (but not inferred functional domains; Figs. 2, 4). A similar pattern of paralogy has been reported in other gene families in multiple spider species, as well as scorpions. For example, duplicated copies of the Hox genes *Deformed*, *Sex combs reduced*, and *Ultrabithorax* were initially identified in the spider *Cupiennius salei* (Schwager et al., 2007), and every paralog had a distinct expression boundary. Appendage patterning genes like *homothorax*, *extradenticle*, and *dachshund* are similarly duplicated, and demonstrably differ at least in expression patterns, if not also in function, in multiple spider species (Prpic et al., 2003; Pechmann and Prpic, 2009; Turetzek et al., 2015). Recently, large-scale duplication of the scorpion Hox cluster was similarly reported in *Mesobuthus martensii* and *Centruroides sculpturatus* (Sharma et al., 2014b; Di et al., 2015), and we previously showed that *C. sculpturatus*, like spiders, have unique expression boundaries for each paralog in the opisthosomal Hox group (Sharma et al., 2014b). Furthermore, analysis of Hox gene trees using a gene tree reconciliation approach supported ancient duplication in the scorpion tree of life, dating at least to the scorpion common ancestor (Sharma et al., 2015b, 2015c). Beyond developmental patterning genes, neuropeptides of spiders and scorpions (Veenstra, 2016) and microRNAs of these groups (Leite et al., 2016) also demonstrate comparable patterns of duplication, suggesting that such duplications are systemic in a subset of Chelicerata. In contrast, distantly related arachnid orders (e.g., mites, harvestmen), as well as Mandibulata, all bear single copy orthologs for genes reported as duplicated in spiders and scorpions (Grbić et al., 2011; Sharma et al., 2012a, 2012b; Veenstra, 2016).

These results also accord with recent phylogenomic results that support the Arachnopulmonata hypothesis (a clade consisting of scorpions, spiders, Amblypygi, Uropygi, and Schizomida—all the arachnid orders with book lungs, and excluding such taxa as harvestmen, mites, and ticks; Sharma et al., 2014a). The sum of these data may be consistent with a scenario of ancient and extensive genome duplication (partial or whole) in the common ancestor of Arachnopulmonata, to the exclusion of other arachnids. As was the case for individual Hox gene tree analyses (Sharma et al., 2014b), the *ss* gene tree has low nodal support for the placement of the two spider paralogs within the arachnid clade, a result partly attributable to fragmentary sequences from transcriptomic datasets (Fig. 2). The degree of pairwise sequence divergence in the five arachnid *ss* homologs is consistent with an ancient age of divergence of the arachnopulmonate paralogs.

### 4.2. *ss* expression and function across Mandibulata suggests a conserved role as a flagellar determinant

Consistent with the prediction that *ss* is a determinant of the flagellum (the distal part of the antenna) throughout Mandibulata, we observed strong expression of *ss* orthologs throughout the distal antenna of mandibulate exemplars, regardless of each lineage's adult antennal morphology. *Oncopeltus fasciatus* was selected for the plesiomorphic nature of its antennal morphology, life history (hemimetaboly) and tarsal formula (two tarsomeres on each leg, in contrast to the five in *Drosophila* and *Tribolium*). *Parhyale hawaiensis* was selected to represent the typical crustacean condition of two antennal

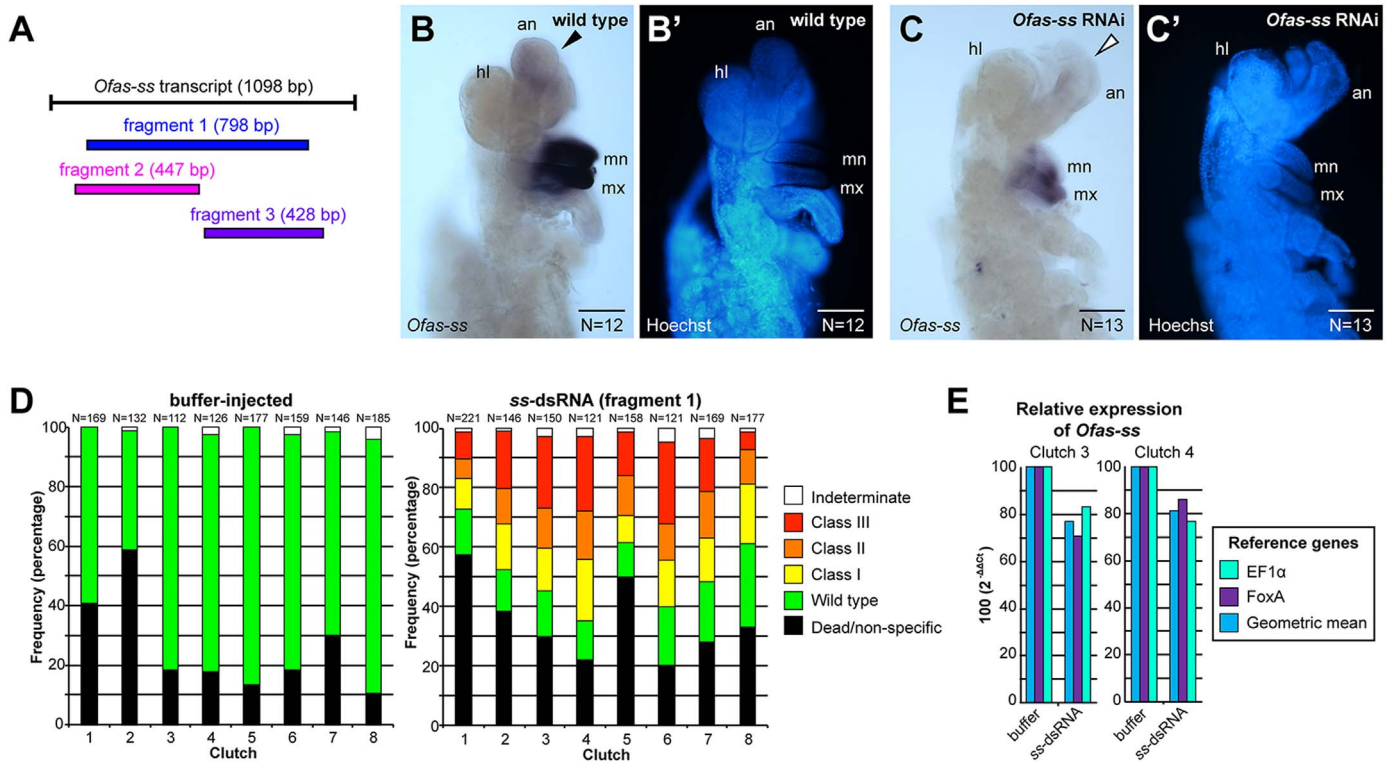


**Fig. 6.** Experimental design and execution of *Ofas-ss*-RNAi. (A) Distribution and lengths of cDNA fragments amplified for RNAi. (B) Expression of *Ofas-ss* in a wildtype embryo (third clutch) ca. 80 hAEL in lateral view. Black arrowhead indicates expression; non-specific staining is observed at this stage in the mandible and maxilla. (C) Expression of *Ofas-ss* in embryo ca. 80 hAEL from a fragment 1 knockdown experiment (third clutch) in lateral view, showing reduced expression in the homeotically transformed distal antenna. (D) Distribution of phenotypes in negative control (left) and *Ofas-ss*-RNAi experiments (842-bp fragment). Colors correspond to the legend indicated to the right. (E) Verification of *Ofas-ss* knockdown via qPCR for clutch 3 (left) and clutch 4 (right) embryos fixed 72 h AEL. Blue bars indicate geometric mean of RQ values based on FoxK (purple) and EF1α(cyan). (B'-C') Counterstaining of embryos shown in (B) and (C) with Hoechst 33342. Abbreviations as in Figure 2. Scale bars: 100 μm.

pairs (a deutocerebral and tritocerebral pair). *Lithobius atkinsoni* was selected to represent Myriapoda, the sister group to the remaining Mandibulata. We observed expression of *ss* throughout the distal territories of all limb buds that will develop a flagellar (distal antennal) identity. Other expression domains comparable to those of *Dmel-ss* and *Tcas-ss* in late stages were also observed in *P. hawaiensis*, namely, in the maxillae, at the base of the coxa-trochanter joint of posterior trunk appendages, and in the presumptive peripheral nervous system (Fig. 3E). The functional significance of these domains is unknown, as they are not associated with a *ss* loss-of-function phenotype in *Drosophila* or *Tribolium* (Duncan et al., 1998; Shippy et al., 2008; Toegel et al., 2009).

We conducted parental RNAi against *Ofas-ss* to test whether strong expression of an *ss* ortholog in deutocerebral limb buds corresponds to a conserved function as a distal antennal determinant, in an organism where (a) antennal identity is conferred only once, during embryogenesis, and (b) antennal morphology is simple and postembryonic development consists only of allometric growth of the four antennal articles. Our results suggest that *ss* is a *bona fide* distal antennal determinant in this hemimetabolous insect. The antennal morphology of Class III phenotypes in this study is remarkably similar to the effects of larval RNAi against *Tcas-ss* (Shippy et al., 2008) or null mutants of *Dmel-ss* (Duncan et al., 1998), wherein the entire appendage is reduced in length, bears a pair of tarsal claws at the distal terminus, and lacks sensory structures in the affected area.

Beyond the data generated herein, expression of *ss* has been surveyed in abnormally developing embryos of the millipede *Glomeris marginata* (Janssen, 2013) and in the onychophoran *Euperipatoides kanangrensis* (Oliveira et al., 2014). In *Glomeris* embryos with duplicated posterior germbands, *ss* was strongly expressed in the antennal and maxillary limb buds, and in some cases, also weakly expressed in all trunk appendages (Figs. 2E and 3A of Janssen, 2013). As wild type expression of *Gmar-ss* was not shown in that study, these data are difficult to compare to the mandibulate data generated herein. In the onychophoran, expression of *ss* occurs in the frontal (protocerebral) appendages as rings of alternating expression strength, corresponding to the annulation of this appendage. Expression also occurs distally in the ectoderm of the other appendages (Oliveira et al., 2014). The rings of expression in the frontal appendages of onychophoran embryos may be comparable to those in the tarsomeres of *Phalangium opilio* walking legs (Fig. 4J, 4K), and possibly reflect a conserved role for *ss* in patterning the distal annulation of appendages across Panarthropoda.

### 4.3. *ss* orthologs are not expressed in the distal cheliceral limb buds of the spider and the harvestman

We predicted that if *ss* were a distal deutocerebral appendage determinant more broadly, *ss* expression in the arachnid chelicera would resemble antennal expression in mandibulate counterparts (i.e., early and strong expression throughout all cells of the distal cheliceral territory). However, none of the arachnid *ss* orthologs was expressed in a comparable manner throughout the developing cheliceral (deutocerebral) limb bud (Fig. 4). Expression in the chelicerae was restricted to a dorso-medial region of the developing appendage, which does not accord with an expression pattern expected for a distal cheliceral determinant. Efforts to knock down expression of either spider *ss* paralog alone, or both paralogs together, did not produce a cheliceral or tarsal phenotype, in spite of reduction of expression signal in single- and double-knockdown experiments (Supplementary Fig. 1). In our positive control experiment, we replicated a gap phenotype with high (> 90%) knockdown efficiency in hatchlings via parental RNAi against *Ptep-Dll* (Supplementary Fig. 1). Together with the lack of *ss* expression throughout the distal chelicera, these data suggest that *ss* is not required for cheliceral identity in arachnids.

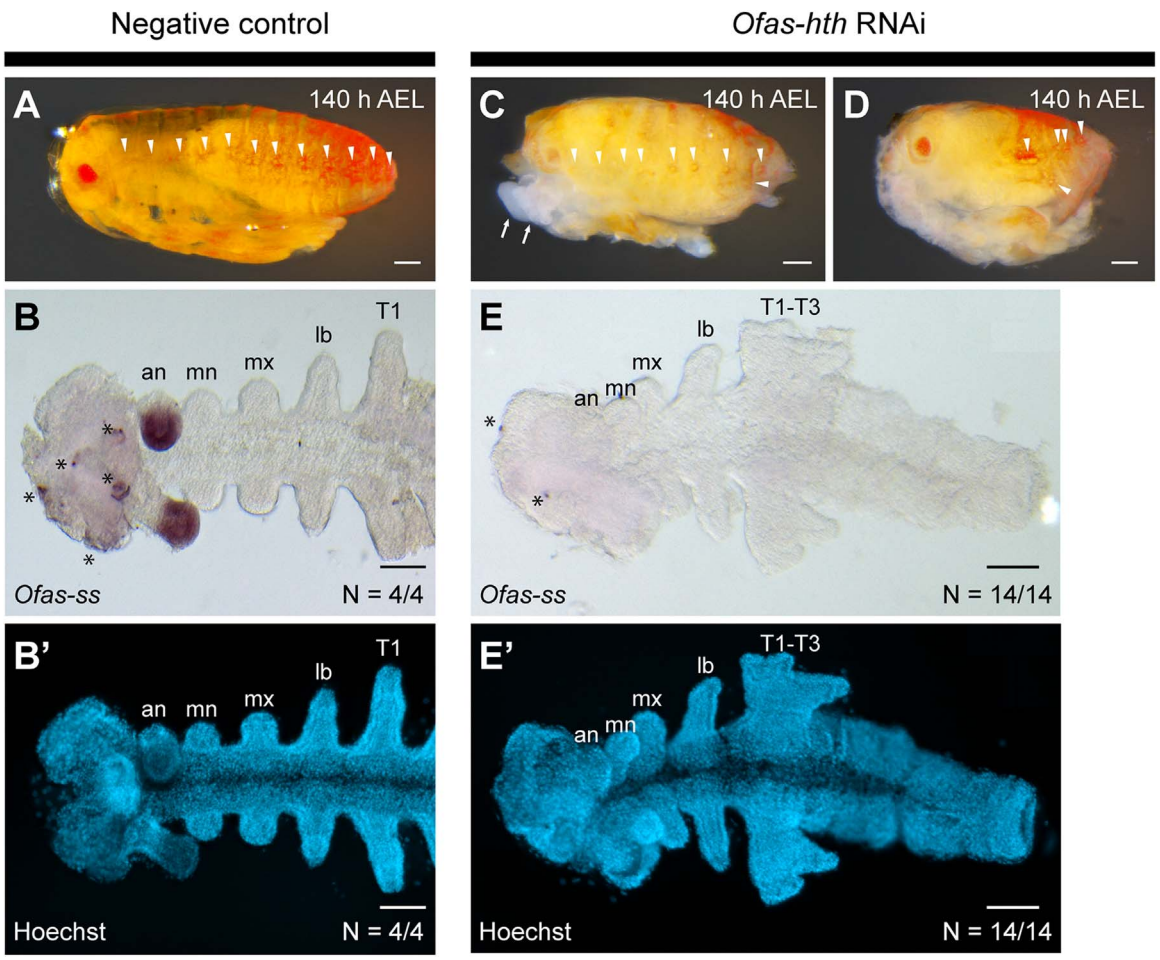


**Fig. 7.** Inference of regulation of *Ofas-ss* by *Ofas-hth*. (A) Wild type late-stage O. fasciatus embryo in lateral view. (B) Wild type expression of *Ofas-ss* in the head segments, 72 h AEL. (C, D) Late stage embryos in lateral view from fifth and sixth clutches of a *Ofas-hth* dsRNA-injected female. Note the reduced eye in (C) and the fused spiracles in (D). (E) Expression of *Ofas-ss* in embryo of a *Ofas-hth* dsRNA-injected female, 72 h AEL; note the fused T1-T3 appendages. White arrowheads in (A), (C), and (D) indicate openings of spiracles (one pair per segment, from T2 to A10). White arrows in C indicate fusion antennal and mandibular appendages. Asterisks indicate non-specific staining (membrane) in (B) and (E). (E' and E') Counterstaining of embryos shown in (B) and (E) with Hoechst 33342. Abbreviations as in Figure 3. All scale bars are 100 μm.

However, as it is not possible to rule out gene function based upon RNAi-mediated knockdowns, our data may alternatively be interpreted to correspond to inefficiency of parental RNAi in knocking down expression of genes expressed late in spider development. As an example, parental RNAi against *Ptep-Distal-less* induces a gap phenotype, corresponding to an early function of this gene, but in most embryos, the remaining body segments form wild type appendages, due to reactivation of *Dll* expression in later stages (Pechmann et al., 2011; this study, Supplementary Fig. 1). In that study of *Ptep-Dll*, only embryonic RNAi against *Ptep-Dll* achieved the classic limbless phenotype, corresponding to knockdown of *Dll* expression in later stages, albeit with remarkably low (ca. 3%) efficiency as measured by completely limbless phenotypes (Pechmann et al., 2011). Regardless, we note that *ss* expression in arachnids deviates from the pattern expected for a cheliceral selector gene, i.e., expression throughout all of the cells of the distal portion of the cheliceral axis in stages prior to specification of cheliceral identity (compare Figs. 3 and 4). We therefore consider it unlikely that *ss* is a distal cheliceral determinant.

In contrast to *Parasteatoda*, embryos of *Phalangium* injected under oil are capable of hatching, and bear tarsal claws (pedipalp and walking leg landmarks) as first instars, which has previously enabled interpretation of experimentally-induced homeosis (Sharma et al., 2013, 2015a). Future investigations of *ss* in arachnids should therefore interrogate the function of the single *ss* ortholog in the harvestman *Phalangium opilio* to corroborate the results obtained with the two spider paralogs (see below).

While not examined here, we further note that upstream regulation of *ss* differs in insects and arachnids. In insects, *ss* is regulated by the Hox gene *Antennapedia* (*Antp*), which is generally expressed in the thoracic (leg-bearing) segments (reviewed by Hughes and Kaufman (2002)). Knockdown phenotypes or null mutants of *Antp* of multiple insects display homeotic leg-to-antenna transformations (Shippy et al., 2008; Emmons et al., 2007; Duncan et al., 2010), including in *Oncopeltus* (Angelini et al., 2005). By contrast, arachnid *Antp* orthologs are always expressed in the opisthosoma (the posterior, limbless tagma of Euchelicerata; Damen et al., 1998; Telford and Thomas, 1998; Sharma et al., 2012b; Santos et al., 2013; Sharma et al., 2014b) and knockdown of *Antp* in *Parasteatoda* results in de-repression of legs on the first opisthosomal segment (Khadjeh et al., 2012). Rather, Hox regulation of appendage identity in *Parasteatoda* at least partly involves *Deformed-1* (*Dfd-1*); a knockdown of this paralog results in restriction of the expression domain of *hth-1* in the first walking leg, and homeotic transformation of the first walking leg to pedipalp identity (Pechmann et al., 2015). Given the highly conserved expression domains of the anterior group of Hox genes as well as *hth* in the prosoma of arachnids (Telford and Thomas, 1998; Sharma et al., 2012a, 2015a), it is likely that regulation of arachnid *hth* by *Dfd* is conserved across Arachnida. To date, transcriptional regulation of arachnid *hth* orthologs has not been explored.

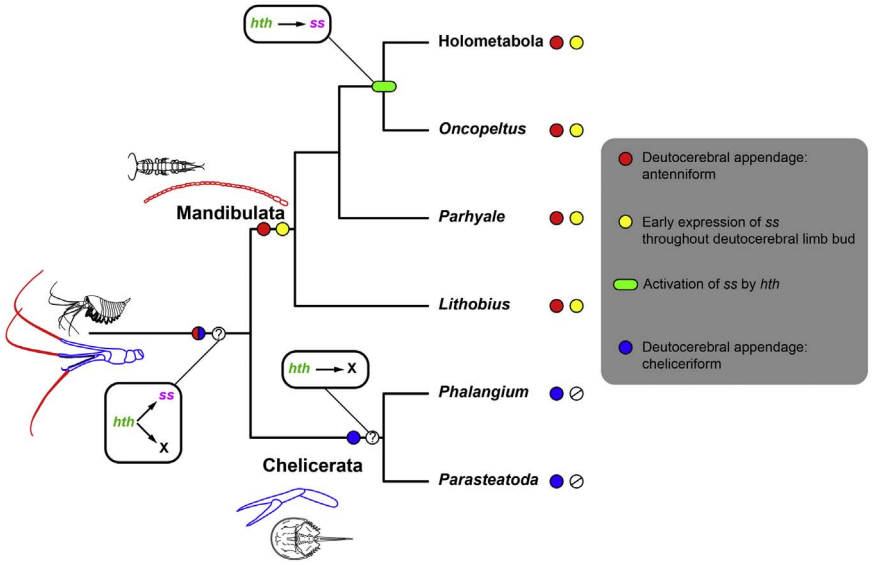


**Fig. 8.** Model of deutocerebral appendage evolution at the base of Arthropoda. Inferred ancestral appendage corresponds to deutocerebral appendage of the fossil leanchoiliid Yawunik kootenayi (redrawn from Aria et al., 2015; based on phylogeny of Legg et al., 2013). Blue portions indicate cheliceriform elements; red portions indicate flagellar/antennal elements. Circles indicate character states, as indicated on the right. "X" denotes unknown cheliceral determinant(s).

### *4.4. ss may underlie convergent evolution of tarsomeres in distantly related arthropod lineages*

The terminal podomere (tarsus or dactylus) is putatively homologous across Arthropoda and the condition of an undivided tarsus is considered ancestral, as inferred from parsimony-based ancestral state reconstructions and early arthropod appendages in the fossil record (Tajiri et al., 2011). However, tarsomeres have evolved repeatedly in unrelated lineages, including derived insects, scutigeromorph centipedes, and several orders of arachnids (Tajiri et al., 2011; Edgecombe and Giribet, 2006, 2007).

In *Drosophila*, null *ss* mutants display defects in tarsomere development (loss of tarsomeres 2–4). Larval RNAi against *Tcas-ss* similarly results in adult beetles with fused or missing tarsomeres. In *Oncopeltus*, which reflects the plesiomorphic condition of a two-segmented tarsus observed in many hemimetabolous insects, no defects in tarsomere number or morphology were observed even in Class III embryos (Fig. 5), suggesting that the function of *ss* in patterning the tarsal field in late stages of holometabolous appendage development represents a derived condition.

*Parasteatoda* and *Phalangium* thus represent an independent case of tarsomere evolution within arthropods, with the former bearing an undivided tarsus, and the latter bearing a unique number of tarsomeres on every walking leg (the pedipalpal tarsus is undivided in both species). The hatchling of *Phalangium* bears the fewest (12) tarsomeres on leg I and the most (24) leg II, but these numbers increase across postembryonic development (Bachmann and Schaefer, 1983). In some groups of harvestmen, tarsal formula is variable to the level of species groups and is used as a diagnostic character in harvestman systematics (Pinto-da-Rocha and Giribet, 2007; Sharma et al., 2009, 2017; Sharma and Giribet (2009)). It is therefore intriguing that the expression pattern of *Popi-ss* during embryogenesis differs in each walking leg tarsus, relative to the pedipalpal tarsus. The strong positive correlation we observed between the number of *Popi-ss* expression bands in the developing tarsi and the number of tarsomeres borne by those tarsi suggests that this gene may have been independently recruited to the terminal leg patterning pathway in insects and arachnids. Future tests of this hypothesis should therefore examine embryonic RNAi against *Popi-ss*, with a concomitant test of function associated with the dorsomedial cheliceral expression domain (Fig. 4).

## 5. Conclusion

Taken together, our expression surveys and functional results support a hypothesis of divergence of downstream targets of *hth* in the deutocerebral appendage of Mandibulata and Chelicerata (Fig. 8), and suggest that *ss* may be a flagellar determinant more broadly. Given the absence of functional tools in Myriapoda, future tests of this hypothesis should focus on the two antennal pairs of such crustacean exemplars as *Parhyale*, with the prediction that knockdown of *Phaw-ss* will result in distal antenna-to-leg transformations in both the deutocerebral and the tritocerebral antenna. The identity of the chelicera-specific determinant(s) remains unknown, but expression patterns of arachnid *ss* orthologs suggest that *ss* is not among them.

## Acknowledgments

We are indebted to Tripti Gupta for her help with in situ hybridization in *Parhyale hawaiensis*. Comments from Georg Brenneis improved an early draft of this work. Early logistical support at UW-Madison was generously provided to PPS by Kurt Amann, Yevgenya Grinblat, and Tony Stretton. Comments from the editor, Claude Desplan, and two anonymous reviewers improved an earlier draft of the manuscript. This work was supported by internal AMNH funds to WCW, National Science Foundation grant IOS-1257217 to CGE, and National Science Foundation grant IOS-1552610 to PPS.

## Appendix A. Supporting information

Supplementary data associated with this article can be found in the online version at doi:10.1016/j.ydbio.2017.07.016.

## References

Akiyama-Oda, Y., Oda, H., 2003. Early patterning of the spider embryo: a cluster of mesenchymal cells at the cumulus produces Dpp signals received by germ disc epithelial cells. Development 130, 1735–1747. http://dx.doi.org/10.1242/dev.00390.

Angelini, D.R., Kaufman, T.C., 2004. Functional analyses in the hemipteran *Oncopeltus fasciatus* reveal conserved and derived aspects of appendage patterning in insects. Dev. Biol. 271, 306–321. http://dx.doi.org/10.1016/j.ydbio.2004.04.005.

Angelini, D.R., Liu, P.Z., Hughes, C.L., Kaufman, T.C., 2005. Hox gene function and interaction in the milkweed bug *Oncopeltus fasciatus* (Hemiptera). Dev. Biol. 287, 440–455. http://dx.doi.org/10.1016/j.ydbio.2005.08.010.

Aria, C., Caron, J.-B., Gaines, R., 2015. A large new leanchoiliid from the Burgess Shale and the influence of inapplicable states on stem arthropod phylogeny. Palaeontology 58, 629–660. http://dx.doi.org/10.1111/pala.12161.
Bachmann, E., Schaefer, M., 1983. Notes on the life cycle of *Phalangium opilio* (Opiliones). Verh. Naturw. Ver. Hamb. 26, 255–263.
Borner, J., Rehm, P., Schill, R.O., Ebersberger, I., Burmester, T., 2014. A transcriptome approach to ecdysozoan phylogeny. Mol. Phylogenet. Evol. 80, 79–87. http://dx.doi.org/10.1016/j.ympev.2014.08.001.
Boxshall, G.A., 2004. The evolution of arthropod limbs. Biol. Rev. 79, 253–300. http://dx.doi.org/10.1017/S1464793103006274.
Brenneis, G., Ungerer, P., Scholtz, G., 2008. The chelifores of sea spiders (Arthropoda, Pycnogonida) are the appendages of the deutocerebral segment. Evol. Dev. 10, 717–724. http://dx.doi.org/10.1111/j.1525-142X.2008.00285.x.
Browne, W.E., Price, A.L., Gerberding, M., Patel, N.H., 2005. Stages of embryonic development in the amphipod crustacean, *Parhyale hawaiensis*. Genesis 42, 124–149. http://dx.doi.org/10.1002/gene.20145.
Campbell, L.I., Rota-Stabelli, O., Edgecombe, G.D., Marchioro, T., Longhorn, S.J., Telford, M.J., Philippe, H., Rebecchi, L., Peterson, K.J., Pisani, D., 2011. MicroRNAs and phylogenomics resolve the relationships of Tardigrada and suggest that velvet worms are the sister group of Arthropoda. Proc. Natl. Acad. Sci. USA 108, 15920–15924.
Chen, J., Waloszek, D., Maas, A., 2004. A new "great-appendage"arthropod from the Lower Cambrian of China and homology of chelicerate chelicerae and raptorial antero-ventral appendages. Lethaia 37, 3–20. http://dx.doi.org/10.1080/00241160410004764.
Chipman, A.D., 2015. An embryological perspective on the early arthropod fossil record. BMC Evol. Biol. 15, 285.
Chipman, A.D., Ferrier, D.E.K., Brena, C., Qu, J., Hughes, D.S.T., et al., 2014. The first myriapod genome sequence reveals conservative arthropod gene content and genome organisation in the centipede *Strigamia maritima*. PLOS Biol. 12, e1002005 . http://dx.doi.org/10.1371/journal.pbio.1002005.s072.
Daley, A.C., Budd, G.E., Caron, J.-B., Edgecombe, G.E., Collins, D., 2009. The burgess shale Anomalocaridid *Hurdia* and its significance for early euarthropod evolution. Science 323, 1597–1600.
Damen, W.G.M., Hausdorf, M., Seyfarth, E.A., Tautz, D., 1998. A conserved mode of head segmentation in arthropods revealed by the expression pattern of Hox genes in a spider. Proc. Natl. Acad. Sci. USA 95, 10665–10670.
de Celis Ibeas, J., Bray, S., 2003. Bowl is required downstream of Notch for elaboration of distal limb patterning. Development 130, 5943–5952.
Di, Z., Yu, Y., Wu, Y., Hao, P., He, Y., Zhao, H., Li, Y., Zhao, G., Li, X., Li, W., Cao, Z., 2015. Genome-wide analysis of homeobox genes from *Mesobuthus martensii* reveals Hox gene duplication in scorpions. Insect Biochem. Mol. Biol. 61, 25–33.
Dong, P.D., Chu, J., Panganiban, G., 2001. Proximodistal domain specification and interactions in developing *Drosophila* appendages. Development 128, 2365–2372.
Dong, P.D.S., Dicks, J.S., Panganiban, G., 2002. *Distal-less* and *homothorax* regulate multiple targets to pattern the *Drosophila* antenna. Development 129, 1967–1974.
Duncan, D., Kiefel, P., Duncan, I., 2010. Control of the *spineless* antennal enhancer: direct repression of antennal target genes by Antennapedia. Dev. Biol. 347, 82–91. http://dx.doi.org/10.1016/j.ydbio.2010.08.012.
Duncan, D.M., Burgess, E.A., Duncan, I., 1998. Control of distal antennal identity and tarsal development in *Drosophila* by *spineless-aristapedia*, a homolog of the mammalian dioxin receptor. Genes Dev. 12, 1290–1303.
Edgar, R.C., 2004. MUSCLE: multiple sequence alignment with high accuracy and high throughput. Nucleic Acids Res. 32, 1792–1797. http://dx.doi.org/10.1093/nar/gkh340.
Edgecombe, G.E., Giribet, G., 2006. A century later–a total evidence re-evaluation of the phylogeny of scutigeromorph centipedes (Myriapoda: Chilopoda). Invertebr. Syst. 20, 503–525.
Edgecombe, G.E., Giribet, G., 2007. Evolutionary Biology of Centipedes (Myriapoda: Chilopoda). Ann. Rev. Entomol. 52, 151–170.
Edgecombe, G.E., Legg, D., 2014. Origins and early evolution of arthropods. Palaeontology 57, 457–468.
Emerald, B., Cohen, S., 2004. Spatial and temporal regulation of the homeotic selector gene *Antennapedia* is required for the establishment of leg identity in *Drosophila*. Dev. Biol. 267, 462–472. http://dx.doi.org/10.1016/j.ydbio.2003.12.006.
Emmons, R.B., Duncan, D., Duncan, I., 2007. Regulation of the *Drosophila* distal antennal determinant *spineless*. Dev. Biol. 302, 412–426. http://dx.doi.org/10.1016/j.ydbio.2006.09.044.
Godt, D., Couderc, J.L., Cramton, S.E., Laski, F.A., 1993. Pattern-formation in the limbs of *Drosophila*: *bric à brac* is expressed in both a gradient and a wave-like pattern and is required for specification and proper segmentation of the tarsus. Development 119, 799–812.
Grbić, M., Van Leeuwen, T., Clark, R.M., Rombauts, S., Rouzé, P., et al., 2011. The genome of *Tetranychus urticae* reveals herbivorous pest adaptations. Nature 479, 487–492. http://dx.doi.org/10.1038/nature10640.
Haug, J.T., Waloszek, D., Maas, A., Liu, Y., Haug, C., 2012. Functional morphology, ontogeny and evolution of mantis shrimp-like predators in the Cambrian. Palaeontology 55, 369–399.
Hughes, C., Kaufman, T., 2002. Hox genes and the evolution of the arthropod body plan. Evol. Dev. 4, 459–499.
Jager, M., Murienne, J., Clabaut, C., Deutsch, J., Guyader, H.L., Manuel, M., 2006. Homology of arthropod anterior appendages revealed by Hox gene expression in a sea spider. Nature 441, 506–508. http://dx.doi.org/10.1038/nature04591.
Janssen, R., 2013. Developmental abnormalities in *Glomeris marginata* (Villers 1789) (Myriapoda: diplopoda): implications for body axis determination in a myriapod. Naturwissenschaften 100, 33–43.
Kadner, D., Stollewerk, A., 2004. Neurogenesis in the chilopod *Lithobius forficatus* suggests more similarities to chelicerates than to insects. Dev. Genes Evol. 214, 367–379. http://dx.doi.org/10.1007/s00427-004-0419-z.
Khadjeh, S., Turetzek, N., Pechmann, M., Schwager, E.E., Wimmer, E.A., Damen, W.G.M., Prpic, N.-M., 2012. Divergent role of the Hox gene *Antennapedia* in spiders is responsible for the convergent evolution of abdominal limb repression. Proc. Natl. Acad. Sci. USA 109, 4921–4926. http://dx.doi.org/10.1073/pnas.1116421109.
Kühl, G., Briggs, D.E.G., Rust, J., 2009. A great-appendage arthropod with a radial mouth from the Lower Devonian Hunsrück Slate, Germany. Science 323, 771–773.
Legg, D.A., Sutton, M.D., Edgecombe, G.D., 2013. Arthropod fossil data increase congruence of morphological and molecular phylogenies. Nat. Commun. 4, 2485. http://dx.doi.org/10.1038/ncomms3485.
Leite, D.J., Ninova, M., Hilbrant, M., Arif, S., Griffith-Jones, S., Ronshaugen, M., McGregor, A.P., 2016. Pervasive microRNA duplication in chelicerates: insights from the embryonic microRNA repertoire of the spider *Parasteatoda tepidariorum*. Genome Biol. Evol. 8, 2133–2144. http://dx.doi.org/10.1093/gbe/evw143.
Liu, P., Kaufman, T.C., 2009. In situ hybridization of large milkweed bug (*Oncopeltus*) tissues. CSH Protoc. 2009 (4), 1–4. http://dx.doi.org/10.1101/pdb.prot5262.
Ma, X., Hou, X., Edgecombe, G.D., Strausfeld, N.J., 2012. Complex brain and optic lobes in an early Cambrian arthropod. Nature 490, 258–262.
Mittmann, B., Wolff, C., 2012. Embryonic development and staging of the cobweb spider *Parasteatoda tepidariorum* C. L. Koch, 1841 (syn.: *Achaearanea tepidariorum*; Araneomorphae; Theridiidae). Dev. Genes Evol. 222, 189–216. http://dx.doi.org/10.1007/s00427-012-0401-0.
Oliveira, M.B., Liedholm, S.E., Lopez, J.E., Lochte, A.A., Pazio, M., Martin, J.P., Mörch, P.R., Salakka, S., York, J., Yoshimoto, A., Janssen, R., 2014. Expression of arthropod distal limb-patterning genes in the onychophoran *Euperipatoides kanangrensis*. Dev. Genes. Evol. 224, 87–96.
Pechmann, M., Khadjeh, S., Turetzek, N., Mcgregor, A.P., Damen, W.G.M., Prpic, N.-M., 2011. Novel function of *Distal-less* as a gap gene during spider segmentation. PLoS Genet. 7, e1002342. http://dx.doi.org/10.1371/journal.pgen.1002342.g004.
Pechmann, M., Prpic, N.-M., 2009. Appendage patterning in the South American bird spider *Acanthoscurria geniculata* (Araneae: mygalomorphae). Dev. Genes Evol. 219, 189–198. http://dx.doi.org/10.1007/s00427-009-0279-7.
Pechmann, M., Schwager, E.E., Turetzek, N., Prpic, N.-M., 2015. Regressive evolution of the arthropod tritocerebral segment linked to functional divergence of the Hox gene *labial*. Proc. R. Soc. Lond. B 282. http://dx.doi.org/10.1098/rspb.2015.1162, (20151162).
Pinto-da-Rocha, R., Giribet, G., 2007. Taxonomy. In: Pinto-da-Rocha, R., Machado, G., Giribet, G. (Eds.), Harvestmen: The Biology of Opiliones. Cambridge University Press, Cambridge, US, 88–246.
Prpic, N.-M., Janssen, R., Wigand, B., Klingler, M., Damen, W., 2003. Gene expression in spider appendages reveals reversal of *exd/hth* spatial specificity, altered leg leg gap gene dynamics, and suggests divergent distal morphogen signaling. Dev. Biol. 264, 119–140.
Rehm, E.J., Hannibal, R.L., Chaw, R.C., Vargas-Vila, M.A., Patel, N.H., 2009. In situ hybridization of labeled RNA probes to fixed *Parhyale hawaiensis* embryos. CSH Protoc. 4, 1–5. http://dx.doi.org/10.1101/pdb.prot5130.
Ronco, M., Uda, T., Mito, T., Minelli, A., Noji, S., Klingler, M., 2008. Antenna and all gnathal appendages are similarly transformed by *homothorax* knock-down in the cricket Gryllus bimaculatus. Dev. Biol. 313, 80–92. http://dx.doi.org/10.1016/j.ydbio.2007.09.059.
Santos, V.T., Ribeiro, L., Fraga, A., de Barros, C.M., Campos, E., Moraes, J., Fontenele, M.R., Araújo, H.M., Feitosa, N.M., Logullo, C., da Fonseca, R.N., 2013. The embryogenesis of the tick *Rhipicephalus* (*Boophilus*) *microplus*: the establishment of a new chelicerate model system. Genesis 51, 803–818. http://dx.doi.org/10.1002/dvg.22717.
Scholtz, G., Edgecombe, G.D., 2006. The evolution of arthropod heads: reconciling morphological, developmental and palaeontological evidence. Dev. Genes Evol. 216, 395–415. http://dx.doi.org/10.1007/s00427-006-0085-4.
Schwager, E.E., Schoppmeier, M., Pechmann, M., Damen, W.G.M., 2007. Duplicated Hox genes in the spider *Cupiennius salei*. Front. Zool. 4, 10. http://dx.doi.org/10.1186/1742-9994-4-10.
Schwager, E.E., Sharma, P.P., Clarke, T., Leite, D.J., Wierschin, T., Pechmann, M., Akiyama-Oda, Y., Esposito, L., Arensburger, P., Bechsgaard, J., Bilde, T., Buffry, A., Chao, H., Dinh, H., Doddapaneni, H., Dugan, S., Eibner, C., Extavour, C.G., Funch, P., Garb, J., Gonzalez, V.L., Griffiths-Jones, S., Han, Y., Hayashi, C., Hilbrant, M., Hughes, D.S.T., Janssen, R., Lee, S.L., Maeso, I., Murali, S.C., Muzny, D.M., da Fonseca, R.N., Qu, J., Ronshaugen, M., Schomburg, C., Schönauer, A., Stollewerk, A., Torres-Oliva, M., Turetzek, N., Vanthournout, B., Werren, J., Wolff, C., Worley, K.C., Gibbs, R.A., Coddington, J., Oda, H., Stanke, M., Ayoub, N.A., Damen, W.G.M., Prpic, N.-M., Flot, J.-F., Posnien, N., Richards, S., McGregor, A.P., 2017. The house spider genome reveals a whole genome duplication during arachnid evolution. BMC Biology 15, 62. http://dx.doi.org/10.1186/s12915-017-0399-x.
Sharma, P.P., Fernández, R., Esposito, L., González-Santillán, E., Monod, L., 2015b. Phylogenomic resolution of scorpions reveals multilevel discordance with morphological phylogenetic signal. Proc. R. Soc. Lond. B 282. http://dx.doi.org/10.1093/molbev/mss208, (20142953).
Sharma, P., Giribet, G., 2009. Sandokanid phylogeny based on eight molecular markers—The evolution of a southeast Asian endemic family of Laniatores (Arachnida, Opiliones). Mol. Phylogenet. Evol. 52, 432–447. http://dx.doi.org/10.1016/j.ympev.2009.03.013.
Sharma, P.P., Kaluziak, S.T., Pérez-Porro, A.R., González, V.L., Hormiga, G., Wheeler, W.C., Giribet, G., 2014a. Phylogenomic interrogation of *Arachnida* reveals systemic conflicts in phylogenetic signal. Mol. Biol. Evol. 31, 2963–2984. http://dx.doi.org/10.1093/molbev/msu235.
Sharma, P.P., Santiago, M.A., González-Santillán, E., Monod, L., Wheeler, W.C., 2015c.

Evidence of duplicated Hox genes in the most recent common ancestor of extant scorpions. Evol. Dev. 17, 347–355. http://dx.doi.org/10.1111/ede.12166.
Sharma, P.P., Santiago, M.A., Kriebel, Ricardo, Lipps, Savana M., Buenavente, P.A.C., Diesmos, A.C., Janda, M., Boyer, S.L., Clouse, R.M., Wheeler, W.C., 2017. A multilocus phylogeny of Podoctidae (Arachnida, Opiliones, Laniatores) reveals the disutility of subfamily nomenclature in armored harvestman systematics. Mol. Phylogenet. Evol. 106, 163–174. http://dx.doi.org/10.1016/j.ympev.2016.09.019.
Sharma, P.P., Schwager, E.E., Extavour, C.G., Giribet, G., 2012a. Hox gene expression in the harvestman *Phalangium opilio* reveals divergent patterning of the chelicerate opisthosoma. Evol. Dev. 14, 450–463. http://dx.doi.org/10.1111/j.1525-142X.2012.00565.x.
Sharma, P.P., Schwager, E.E., Extavour, C.G., Giribet, G., 2012b. Evolution of the chelicera: a dachshund domain is retained in the deutocerebral appendage of Opiliones (Arthropoda, Chelicerata). Evol. Dev. 14, 522–533. http://dx.doi.org/10.1111/ede.12005.
Sharma, P.P., Schwager, E.E., Extavour, C.G., Wheeler, W.C., 2014b. Hox gene duplications correlate with posterior heteronomy in scorpions. Proc. R. Soc. Lond. B 281. http://dx.doi.org/10.1016/j.cub.2009.06.061, (20140661).
Sharma, P.P., Schwager, E.E., Giribet, G., Jockusch, E.L., Extavour, C.G., 2013. *Distal-less* and *dachshund* pattern both plesiomorphic and apomorphic structures in chelicerates: RNA interference in the harvestman *Phalangium opilio* (Opiliones). Evol. Dev. 15, 228–242. http://dx.doi.org/10.1111/ede.12029.
Sharma, P.P., Tarazona, O.A., Lopez, D.H., Schwager, E.E., Cohn, M.J., Wheeler, W.C., Extavour, C.G., 2015a. A conserved genetic mechanism specifies deutocerebral appendage identity in insects and arachnids. Proc. R. Soc. Lond. B 282. http://dx.doi.org/10.1098/rspb.2015.0698, (20150698).
Shippy, T.D., Yeager, S.J., Denell, R.E., 2008. The *Tribolium* spineless ortholog specifies both larval and adult antennal identity. Dev. Genes Evol. 219, 45–51. http://dx.doi.org/10.1007/s00427-008-0261-9.
Siveter, D.J., Briggs, D.E.G., Siveter, D.J., Sutton, M.D., Legg, D., Joomun, S., 2014. A Silurian short-great-appendage arthropod. Proc. R. Soc. Lond. B 281, (20132986).
Smith, F.W., Angelini, D.R., Jockusch, E.L., 2014. A functional genetic analysis in flour beetles (Tenebrionidae) reveals an antennal identity specification mechanism active during metamorphosis in Holometabola. Mech. Dev. 132, 13–27. http://dx.doi.org/10.1016/j.mod.2014.02.002.
Stamatakis, A., 2006. RAxML-VI-HPC: maximum likelihood-based phylogenetic analyses with thousands of taxa and mixed models. Bioinformatics 22, 2688–2690.
Stamatakis, A., Hoover, P., Rougemont, J., 2008. A rapid bootstrap algorithm for the RAxML web servers. Syst. Biol. 57, 758–771. http://dx.doi.org/10.1080/10635150802429642.
Struhl, G., 1982. *Spineless-aristapedia*: a homeotic gene that does not control the development of specific compartments in *Drosophila*. Genetics 102, 737–749.
Tajiri, R., Misaki, K., Yonemura, S., Hayashi, S., 2011. Joint morphology in the insect leg: evolutionary history inferred from Notch loss-of-function phenotypes in *Drosophila*. Development 138, 4621–4626. http://dx.doi.org/10.1242/dev.067330.
Tanaka, G., Hou, X., Ma, X., Edgecombe, G.E., Strausfeld, N.J., 2013. Chelicerate neural ground pattern in a Cambrian great appendage arthropod. Nature 502, 364–368.
Telford, M., Thomas, R., 1998. Expression of homeobox genes shows chelicerate arthropods retain their deutocerebral segment. Proc. Natl. Acad. Sci. USA 95, 10671–10675.
Toegel, J.P., Wimmer, E.A., Prpic, N.-M., 2009. Loss of *spineless* function transforms the *Tribolium* antenna into a thoracic leg with pretarsal, tibiotarsal, and femoral identity. Dev. Genes Evol. 219, 53–58. http://dx.doi.org/10.1007/s00427-008-0265-5.
Turetzek, N., Pechmann, M., Schomburg, C., Schneider, J., Prpic, N.-M., 2015. Neofunctionalization of a duplicate *dachshund* gene underlies the evolution of a novel leg segment in arachnids. Mol. Biol. Evol. 33, 109–121. http://dx.doi.org/10.1093/molbev/msv200.
Vargas Jentzsch, I.M., Hughes, D.S.T., Poelchau, M., Robertson, H.M., Benoit, J.B., Rosendale, A.J., Armisén, D., Duncan, E.J., Vreede, B.M.I., Jacobs, C.G.C., Berger, C., Burnett, D.L., Chang, C., Chen, Y.-T., Chipman, A.D., Cridge, A., Crumière, A.J.J., Dearden, P., Erezyilmaz, D.F., Extavour, C.G., Friedrich, M., Horn, T., Hsiao, Y., Jones, J.W., Jones, T.E., Khila, A., Leask, M., Lovegrove, M., Lu, H., Lu, Y., Nair, A., Palli, S.R., Pick, L., Porter, M.L., Refki, P., Rivera Pomar, R., Roth, S., SachsL, Santos, E., Seibert, J., Sghaier, E., Shukla, J.N., Suzuki, Y., Tidswell, O., Traverso, L., van der Zee, M., Viala, S., Richards, S., Panfilio, K.A., 2015. Oncopeltus fasciatus Official Gene set v1.1. Ag Data Commons. http://dx.doi.org/10.15482/USDA.ADC/1173142.
Veenstra, J.A., 2016. Neuropeptide evolution: chelicerate neurohormone and neuropeptide genes may reflect one or more whole genome duplications. Gen. Comp. Endocrinol. 229, 41–55. http://dx.doi.org/10.1016/j.ygcen.2015.11.019.
Yang, J., Ortega-Hernández, J., Butterfield, N.J., Zhang, X., 2013. Specialized appendages in fuxianhuiids and the head organization of early euarthropods. Nature 494, 468–471.
Zeng, V., Villanueva, K.E., Ewen-Campen, B.S., Alwes, F., Browne, W.E., Extavour, C.G., 2011. De novo assembly and characterization of a maternal and developmental transcriptome for the emerging model crustacean *Parhyale hawaiensis*. BMC Genom. 12, 581. http://dx.doi.org/10.1186/1471-2164-12-581.

**Supplementary File 1.** Primer sequences for riboprobe and dsRNA synthesis.

| Locus/primer | Primer Sequence | Length (bp) |
|---|---|---|
| ***Ofas-hth*** | | |
| Ofas_hth_for | 5' – AACTTCTGCCACCGCTACAT – 3' | 569 |
| Ofas_hth_rev | 5' – GTCAGGTGCTGAAACAACCA – 3' | |
| ***Ofas-ss*** | | |
| Ofas_ss_frag1_for | 5' – CCTCAAAGAGTTAATAGGCGGTA – 3' | 798 |
| Ofas_ss_frag1_rev | 5' – TGAGGGGATCACCAAACTTC – 3' | |
| Ofas_ss_5'_frag2_for | 5' – GGGTTCGTCAACTCCCTCTA – 3' | 447 |
| Ofas_ss_5'_frag2_rev | 5' – ACAGTCGGCCTTCCCTATTT – 3' | |
| Ofas_ss_3'_frag3_for | 5' – AAATAGGGAAGGCCGACTGT – 3' | 428 |
| Ofas_ss_3'_frag3_rev | 5' – AGTCTCCGGCTTCCACTTG – 3' | |
| Ofas_ss_qPCR_for | 5' – CTCTCCAGCTGGGGTAAATG – 3' | 194 |
| Ofas_ss_qPCR_rev | 5' – TGAGGGGATCACCAAACTTC – 3' | |
| ***Phaw-ss*** | | |
| Phaw_ss_for | 5' – CTCGTCAGCTACGATCACCA – 3' | 828 |
| Phaw_ss_rev | 5' – GTCCATGGTACGCTTCCCTA – 3' | |
| ***Latk-ss*** | | |
| Latk_ss_for | 5' – CGTTAGGTTCTGGTGCCTTC – 3' | 641 |
| Latk_ss_rev | 5' – TCAGGAAGTCCCGTAGTTGG - 3' | |
| ***Ptep-Dll*** | | |
| Ptep_Dll_for | 5' – ATGCCCAGGCTTACCCTATT – 3' | 819 |
| Ptep_Dll_rev | 5' – TGTCCCATGAGGAGATAGGC – 3' | |
| ***Ptep-ss-1*** | | |
| Ptep_ss1_5'_for | 5' – CAAACCCCAGCAAAAGACAT – 3' | 809 |
| Ptep_ss1_5'_rev | 5' – CTTGGTGCGCACTAGCTACA – 3' | |
| Ptep_ss1_3'_for | 5' – GCCTTCAGCTAAGCAACACC – 3' | 754 |
| Ptep_ss1_3'_rev | 5' – GTTTGACGGAAGATGGTCGT – 3' | |
| ***Ptep-ss-2*** | | |
| Ptep_ss2_5'_for | 5' – TCGAGAAAGATTGAATGCAGAA – 3' | 651 |
| Ptep_ss2_5'_rev | 5' – TCCATTGAGACTAGAGATAAATCCAA – 3' | |
| Ptep_ss2_3'_for | 5' – GGACACAAGGGGAAAACAAC – 3' | 657 |
| Ptep_ss2_3'_rev | 5' – CCATCTGGGTAGGTAGAAAACC – 3' | |
| ***Popi-ss*** | | |
| Popi_ss_for | 5' – AACAGAGCGTCCTCTCCAAA – 3' | 726 |
| Popi_ss_rev | 5' – GTACGCCAGGTCATCGAAAT – 3' | |

| | Total | Wildtype | Dead | Indeterminate | Class I | Class II | Class III |
|---|---|---|---|---|---|---|---|
| **Buffer-injected** | | | | | | | |
| Clutch 1 | 169 | 100 | 69 | 0 | 0 | 0 | 0 |
| Clutch 2 | 132 | 69 | 62 | 1 | 0 | 0 | 0 |
| Clutch 3 | 112 | 98 | 14 | 0 | 0 | 0 | 0 |
| Clutch 4 | 126 | 108 | 16 | 2 | 0 | 0 | 0 |
| Clutch 5 | 177 | 157 | 20 | 0 | 0 | 0 | 0 |
| Clutch 6 | 159 | 139 | 18 | 2 | 0 | 0 | 0 |
| Clutch 7 | 146 | 123 | 22 | 1 | 0 | 0 | 0 |
| Clutch 8 | 185 | 159 | 22 | 4 | 0 | 0 | 0 |
| *Total* | *1206* | *953* | *243* | *10* | *0* | *0* | *0* |
| | | | | | | | |
| ***ss*-dsRNA fragment 1** | | | | | | | |
| Clutch 1 | 221 | 29 | 118 | 2 | 21 | 31 | 20 |
| Clutch 2 | 146 | 20 | 43 | 1 | 18 | 25 | 39 |
| Clutch 3 | 150 | 35 | 43 | 4 | 19 | 15 | 34 |
| Clutch 4 | 121 | 22 | 18 | 3 | 26 | 25 | 27 |
| Clutch 5 | 158 | 21 | 48 | 1 | 36 | 35 | 17 |
| Clutch 6 | 121 | 28 | 23 | 4 | 28 | 19 | 19 |
| Clutch 7 | 169 | 41 | 33 | 4 | 46 | 28 | 17 |
| Clutch 8 | 177 | 49 | 37 | 2 | 53 | 30 | 6 |
| *Total* | *1263* | *245* | *363* | *21* | *247* | *208* | *179* |
| | | | | | | | |
| ***ss*-dsRNA fragment 2** | | | | | | | |
| Clutch 1 | 44 | 0 | 13 | 0 | 14 | 9 | 8 |
| Clutch 2 | 17 | 0 | 8 | 3 | 5 | 1 | 0 |
| Clutch 3 | 15 | 0 | 2 | 0 | 9 | 4 | 0 |
| Clutch 4 | 14 | 0 | 7 | 0 | 5 | 2 | 0 |
| Clutch 5 | 16 | 0 | 16 | 0 | 0 | 0 | 0 |
| Clutch 6 | 10 | 0 | 10 | 0 | 0 | 0 | 0 |
| *Total* | *116* | *0* | *56* | *3* | *33* | *16* | *8* |
| | | | | | | | |
| ***ss*-dsRNA fragment 3** | | | | | | | |
| Clutch 1 | 63 | 0 | 34 | 2 | 0 | 0 | 27 |
| Clutch 2 | 71 | 0 | 26 | 1 | 1 | 9 | 34 |
| Clutch 3 | 53 | 0 | 12 | 3 | 0 | 0 | 38 |
| Clutch 4 | 66 | 0 | 13 | 0 | 8 | 9 | 36 |
| Clutch 5 | 78 | 0 | 52 | 0 | 0 | 0 | 26 |
| Clutch 6 | 113 | 0 | 63 | 0 | 22 | 18 | 10 |
| *Total* | *444* | *0* | *200* | *6* | *31* | *36* | *171* |

| | Total | Wildtype (8 legs) | Dead | Mosaic (7 legs) | Gap (6 legs) |
|---|---|---|---|---|---|
| **Buffer-injected** | | | | | |
| Clutch 2 | 277 | 242 | 35 | 0 | 0 |
| Clutch 3 | 275 | 191 | 84 | 0 | 0 |
| Clutch 4 | 300 | 237 | 63 | 0 | 0 |
| *Total* | *852* | *670* | *182* | *0* | *0* |
| | | | | | |
| ***Ptep-Dll* -dsRNA** | | | | | |
| Clutch 2 | 331 | 10 | 144 | 6 | 171 |
| Clutch 3 | 331 | 0 | 207 | 0 | 124 |
| Clutch 4 | 631 | 7 | 487 | 4 | 133 |
| *Total* | *1293* | *17* | *838* | *10* | *428* |
| *Total* | | | | | |